Ballast for Lifting

A novel lifting method for topsides of offshore platforms

Marieke M.T. Bakker

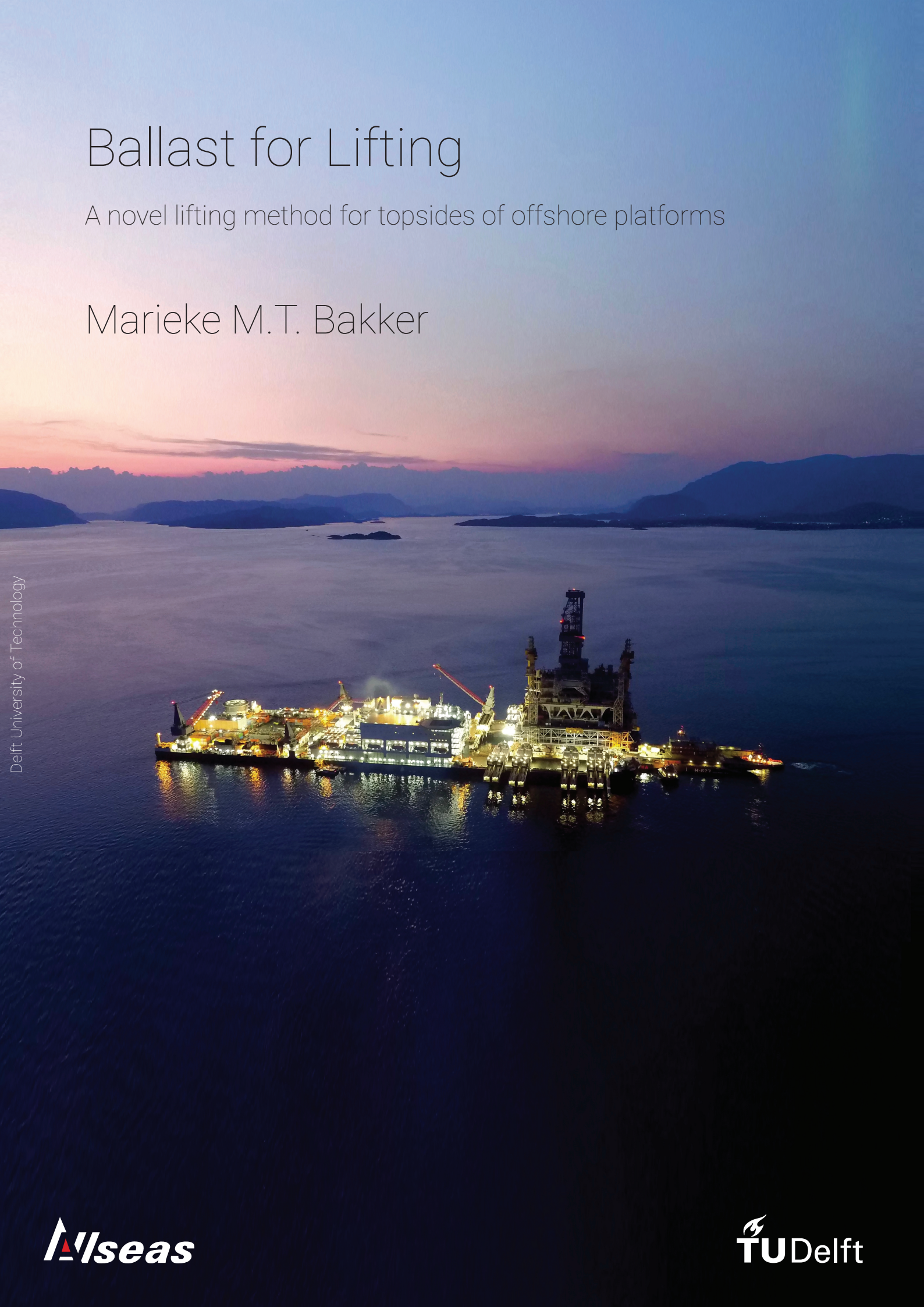

Delft University of Technology

Allseas

TU Delft

Ballast for Lifting
A novel lifting method for topsides of offshore platforms

by

Marieke M.T. Bakker

to obtain the degree of Master of Science in Offshore and Dredging Engineering, specialisation
Floating Offshore Structures
at the Delft University of Technology,
to be defended publicly on Thursday the 5^{th} of December, 2019 at 13:00.

Student number:	4215656	
Project duration:	February, 2019 – December, 2019	
Thesis committee:	Dr. Ir. P. R. Wellens,	TU Delft, Chairman
	Ir. H. Bailly Guimarães,	Allseas, Supervisor
	Ir. M. van der Eijk,	TU Delft, Supervisor
	Dr. B. Atasoy,	TU Delft, 4^{th} committee member
	Dr. Ir. S. K. Advani,	TU Delft, 5^{th} committee member

An electronic version of this thesis is available at `http://repository.tudelft.nl/`.

TU Delft

Abstract

Amazing Grace will be needed for the removal of offshore platforms that are out of *Pioneering Spirit* 's reach. The base case design of *Amazing Grace* is an enlarged version of *Pioneering Spirit* (Figure 1). *Amazing Grace* uses mainly Quick drop Ballast tanks, releasing a lot of water at once, for lifting. *Pioneering Spirit* uses mainly a pneumatic-hydraulic system for fast lifting. The idea is to lift bigger platforms with a less complex system. The behaviour of the base case design of *Amazing Grace* when lifting the upper part of an offshore platform (topside) from its supporting structure (jacket) is studied in this work and the feasibility of the new Quick drop Ballast system is tested.

To perform a feasibility study on lifting topsides with *Amazing Grace* , a set of design requirements is generated. Before using these design requirements, a one tank model is required to simulate the emptying of a tank. The dimensions of an existing *Pioneering Spirit* Quick drop Ballast tank are used. The model is validated by comparing its output to existing physical test data of emptying the same tank. To lift by means of heave only, a bigger volume is used for the one tank model. Once the Quick drop Ballast concept shows to be feasible, the next step is to introduce waves. Waves are modeled using the linear superposition method. An estimation of the time series duration is done by computing the standard deviation of the heave amplitude. For a converged standard deviation, the time series' minimum length needs to be 1200 seconds. The maximum heave amplitude, derived from another statistical analysis, is applied to the connection plateau (when *Amazing Grace* connects and starts lifting the topside without creating clearance). The results show that *Amazing Grace* 's mass, added mass, damping and stiffness (the coefficients of the equation of motion) need to be included to give a more accurate estimation of the dynamics for connecting *Amazing Grace* to the topside and the possible rebounce to the jacket. Although this is a conceptual study, the dynamics are included to get a better understanding of *Amazing Grace* 's response.

To include the previously mentioned coefficients of the equation of motion, the Cummins equation is implemented. The excitation forces are the sum of the wave- and the Quick drop Ballast force. The Quick drop Ballast force is derived from the one tank model. A convergence study shows which time step is needed for this model to work accurately considering its application. The implementation of the Cummins' equation is verified by showing agreement between time- and frequency domain. A sensitivity analysis is used to show the effect of changing the model's main variables. The peak period has the biggest influence on *Amazing Grace* 's heave motion. By varying the coefficients of Cummins' equation in the range of 35.5 - 38 meters draught, the computed vessel motions show that the variation of the draught only has little influence. The Quick drop Ballast system is feasible for both the pretension- and fast lift phase when applying the Quick drop Ballast force at the centre of gravity. The Quick drop Ballast force vector is partly relocated at the bow for applying trim during fast lift. A comparison shows that both the required volume and the number of valves reduce by one third compared to the heave only concept. The maximum allowable trim per length of *Amazing Grace* is 1.5 meter. This maximum is exceeded by 0.2 meters. The 0.2 meters needs to be included for a future topside lift system (TLS) design. It is recommended to apply trim during fast lift since this simplifies the complexity of the Quick drop Ballast system by reducing the required volume of water and the number of valves.

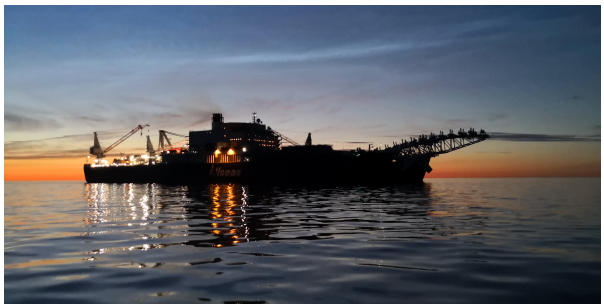

Figure 1: *Pioneering Spirit* , ready for her next adventure

Preface

Being on the water, feeling the waves moving your rowing boat, keeping balance while lifting your rowing blades from the water and trying to get the most sufficient energy transmission to row as fast as possible. It is the beauty of rowing. Apart from rowing, I also appreciate to find some peace and quiet when watching boats pass by at the Oude Maas (Figure 2).

The master thesis you are holding provides the theoretical side of vessels in waves. Vessel motions are calculated as a response to quickly releasing a lot of water using three calculation methods. A more elaborated estimation of what would be happening in real life is gained along the way. By finishing this research, the last assignment for the master Offshore and Dredging Engineering with the specialisation Floating Offshore Structures at TU Delft is completed.

Marieke M.T. Bakker
Delft, November 2019

Figure 2: A visit to the Oude Maas

Acknowledgements

To help me be the best version of myself during the process of graduation, there have been a few people I would like to thank in particular. Thanks to Peter, the head of the graduation committee, the foundation of my research was assured and overall his feedback was extremely helpful. Thank you Helio for being open to questions at any time, for being a sounding board when I needed one and for guiding me through the process whilst letting me discover the tools I needed to fulfill the job. Thank you Naghme, Toni and Mark for confirming the ideas and emotions I had when struggling to find the solutions to my questions. Thank you Bert for your feedback, your technological insights, for showing me around at Pioneering Spirit (Figure 3) and for the laughs we have shared. My parents have also been really supportive although their expertise is in other fields. Thank you mum for trying to grab what I was going through and for giving me the support that was within your reach. Thank you dad for keeping the questions on my thesis flowing although you could not really understand what I was doing all day. Thank you Ilse, my sister, for always trying to be involved with my research and for giving me mental support even when I refused to open up. Thank you Gerry and Jeroen for being the best parents in law I could wish for. Your patience, understanding and interest have helped me to be where I am today. Thank you Arthur for talking me through the process, for showing me the positive side of any setbacks I had, for dragging me outside to make sure I would get some daylight and distraction and for comforting me when I needed it.

I hope you enjoy your reading.

Marieke M.T. Bakker
Delft, November 2019

Figure 3: At the heart of Pioneering Spirit

Contents

Abbreviations

AG	*Amazing Grace*
CIF	Convolution Integral Function
COG	Centre Of Gravity
COR	Centre Of Rotation
DoF	Degrees of Freedom
DP	Dynamic Positioning
HLV	Heavy Lift Vessel
MSL	Mean Sea Level
PS	*Pioneering Spirit*
QdB	Quick drop Ballast
RAO	Response Amplitude Operator
TLS	Topside Lift System

1 Introduction

In offshore engineering the tendency is to go deeper, colder, harsher and older [35]. This urge generates technological challenges. Older upper structures of offshore oil/gas platforms (topsides) are lifted in one piece. Bigger loads create a more adventurous (harsher) job to complete. One of the biggest players in this market is Allseas Group S.A.. This chapter starts with some background on decommissioning offshore platforms. An introduction to Allseas and their biggest vessel *Pioneering Spirit* (PS) is provided. The specifications of the topsides out of PS' reach are identified and the idea of using an even bigger vessel is explained. This leads to a thesis motivation, problem statement and the main objectives of this thesis.

1.1. Background

This section provides some information on decommissioning offshore platforms, it introduces the company Allseas Group S.A., their biggest vessel *Pioneering Spirit* (PS), the lifting phases of PS, PS' Quick drop Ballast (QdB) system, PS' limitations and the future plan to build a bigger vessel: *Amazing Grace* (AG).

1.1.1. Decommissioning offshore platforms

Offshore oil and gas platforms have a lifetime of 30-40 years [40]. After this lifetime, the topside needs to be decommissioned.

Decommissioning can be done in three main ways [9]:

- Piecemeal removal
- Reverse installation
- Single lift

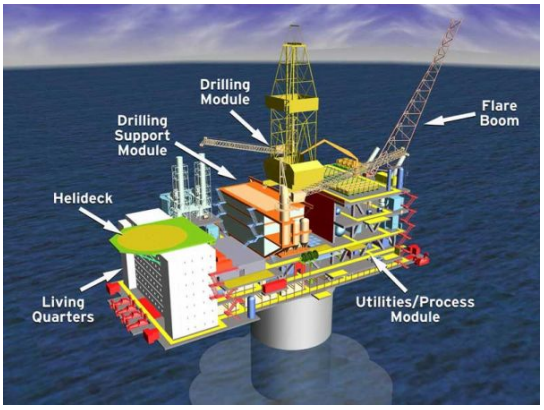

Figure 1.1: Topside modules [3]

Platforms can be removed by taking out pieces of topside modules. Some of the topside modules are shown in Figure 1.1. This method is called piecemeal removal and it involves demolition offshore. Multiple ships and possibly crane vessels are needed for this operation. For reverse installation the platform's modules are moved from the platform to a heavy lift vessel (HLV) in the reverse order of their installation [40]. The reversed installation can be completed by using crane vessels. Semi-submersible-, mono-hull- and jack-up vessels can be used as crane vessels (Figure 1.2). Topsides can be lifted in one go by applying the single lift method. An example of this method is by means of *Pioneering Spirit* (subsection 1.1.3). For reverse installation and the single lift method the HLV is kept in place through suction anchoring (Figure 1.3), embedment anchoring (Figure 1.4) or dynamic positioning (DP). For DP, thrusters are used to stay in place.

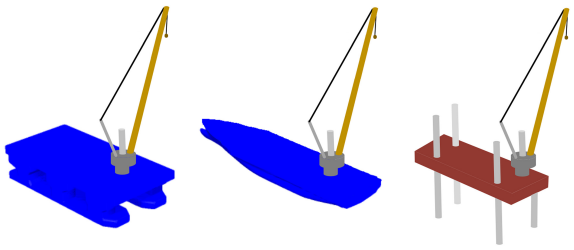

Figure 1.2: Semi-submersible, mono-hull and jack-up vessel [41]

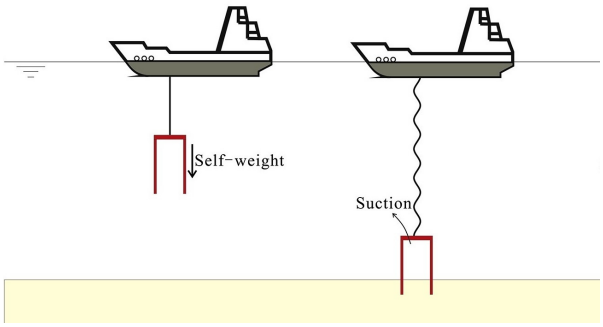

Figure 1.3: Suction anchoring [23]

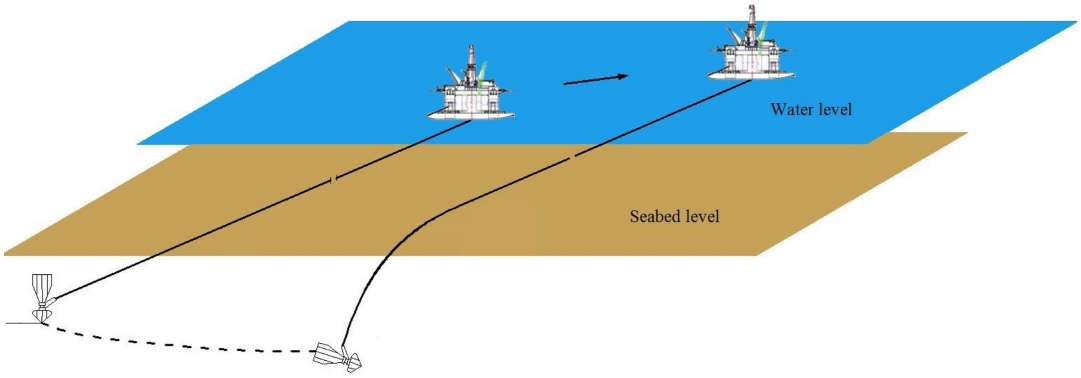

Figure 1.4: Embedment anchoring [15]

1.1.2. Allseas Group S.A.

Allseas is a global leader in subsea construction and offshore pipeline installation. Worldwide over 4000 people are employed by Allseas, operating a fleet of specialised heavy-lift-, pipelay- and support vessels. The vessels are designed and developed in-house.

1.1.3. *Pioneering Spirit* (PS)

Being designed and developed by Allseas, *Pioneering Spirit* (Figure 1.5), is the biggest heavy-lift vessel in the world. She has a dual function of laying record-weight pipelines as well as installing and removing large oil and gas platforms. The topsides of the platforms have a maximum mass of 48,000 tons, being lifted in one go. The substructures of the platforms, jackets, can also be lifted in one piece, reaching a mass of 20,000 tons. The main characteristics of PS are listed in Table 1.1.

Figure 1.5: *Pioneering Spirit*

	Value	[-]
Length hull	382	m
Length between perpendiculars	370	m
Breadth moulded	124	m
Depth moulded	29	m
Draught, scantling	27	m
Draught, operational (typically)	17	m
Draught, transport	13 – 17	m
Draught, transit	12	m
Slot length	122	m
Slot breadth	59	m

Table 1.1: Characteristics *Pioneering Spirit*

Lifting phases – PS

The topside lifting operation of PS can be divided into phases:

- **Transit to platform** – The PS moves towards the location of the offshore platform and increases her draught to such an extend that she remains clear from the underside of the topside.
- **Sail-in [(1) and (2) of Figure 1.6]** – The PS moves in around the substructure of the platform. Once the PS is in position, she will be appropriately deballasted (emptying of ballasting tanks) to achieve the required connecting draught. By using motion compensation, surge, sway and heave are canceled out and the beams may contact the topside.
- **Pretensioning [(2) of Figure 1.6]** – The pretensioning phase starts from the moment the beams are in contact with the topside. After 80% of the topside's load is transferred to the beams, the pretensioning phase is complete.
- **Fast lift [(3) of Figure 1.6]** – The topside is quickly lifted clear from the substructure. The QdB tanks, located at the bows of the PS, are emptied quickly by gravity to make sure the topside does not hit the substructure after being lifted.
- **Sail-out** – During the sail-out, PS moves out with the topside aboard.
- **Transit to shore** – At a safe distance from the substructure of the platform, the topside is secured for transport and PS is ballasted to a transport draught.
- **Transfer topside to barge** – At a sheltered destination near shore, PS offloads the topside onto a cargo barge or dedicated "finger" pier.

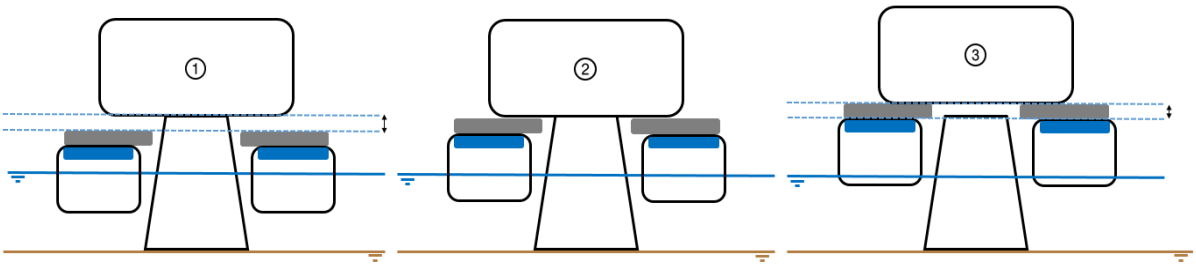

Figure 1.6: Phasing

The QdB system – PS

Pioneering Spirit uses QdB tanks as part of her ballast system. The specifications of the four tanks together are shown in Table 1.2. The main parts of PS' QdB system and their function are described in this subsection.

	Value	[-]
Total water volume	11,100	m^3
Total number of valves	6	
Diameter of valves	2.2	m
Total deballasting time (90% of water volume)	60	$seconds$

Table 1.2: QdB Tanks PS

Pumps are used to supply ballast water through a network of piping. A small butterfly valve is opened to access the tank. The water is stored in the tank until it is needed for deballasting purposes. Two actuators are used for one big butterfly valve to open within 4 seconds. A hydraulic system is used to control the actuators. Ballast water is then released through the fall pipe. The PS has two QdB tanks at each bow. One of the two tanks is bigger than the other. The big tank contains two big butterfly valves and the small tank contains one big butterfly valve. If one of the two valves of the big QdB tank gets stuck during the deballasting operation, the initial heeling offset is accepted and over a period of time the heeling angle goes back to a pre-calculated value. All QdB tanks are empty by then. If the valve of the smaller QdB tank gets stuck, the heeling offset is accepted since this condition is non-hazardous. If two valves of a single big QdB tank get stuck, a back-up hand pump can be used. The QdB tank could also be emptied via the main ballast system. Software is needed to control the filling and discharging of the ballast water tanks. A signal is received for an opened or closed valve.

1.1.4. Platforms

A market research was conducted by Allseas. This research has shown that the topsides that are out of PS' reach have a lower bound for the airgap (gap between mean sea level (MSL) and the underside of the topside) and an upper bound for the mass as follows:

- Airgap: 15 m
- Mass: 72,000 ton

1.1.5. Thesis motivation and *Amazing Grace* (AG)

There will always be relative motions between a fixed platform and a moving ship. When the actual lifting starts, rebouncing the topside to the jacket needs to be prevented. The aim is to quickly lift and increase the platform's height substantially to eliminate the risk of rebouncing. A lot of energy is needed to lift the platform and to create an extra clearance within a limited time frame. For PS, compressed air expands and is used via hydraulic pressure to lift the platform. Hydraulic systems are expensive. For AG, a simpler and comparably fast method is needed to lift the topsides that are out of PS' reach due to their enormous mass and limited airgap. AG is bigger so there will be fewer ship motions. The current idea is to apply only a QdB system, accommodating the full lift. The main characteristics of the new vessel, AG, are listed in Table 1.3.

	Value	[-]
Length hull	400	m
Breadth moulded	187	m
Depth moulded	42	m
Slot length	180	m
Slot breadth	81	m

Table 1.3: Characteristics AG

1.2. Problem statement

Allseas uses PS for installing and decommissioning platforms. A market research has shown that several platforms are out of PS's reach (subsection 1.1.4). To lift a topside with a big mass within a limited time, a lot of energy is needed. Therefore, a QdB system accommodating the full lift has been proposed. This system has to be less complex than the hydraulic system currently used for PS. Various ideas of applications are presented in Appendix A. It has been decided to use the current design of PS' QdB tanks as a starting point. The feasibility of using only QdB tanks for lifting the topside has not been proven yet.

1.3. Research questions and objectives

To solve the above mentioned problem, the research questions consider two subjects: design requirements and a feasibility study of the new QdB system accommodating the full lift. Design requirements are functional attributes that enable an engineering team to convert ideas into design features [28]. The list of design requirements considers sea state variables and the clearance to be created from the jacket within a certain period of time. This list will help to convert the idea of applying the QdB system into design features whilst conducting the feasibility study. The research questions are:

"What are the design requirements for the QdB system?"

"Is it possible to lift topsides using QdB tanks?"

To answer the questions, the research objectives are:

- to simulate the current QdB tank of PS and to validate this model by comparing the output to measurement data provided by Allseas
- to simulate the new QdB system as a one-tank-model
- to define the challenges of using a QdB system for lifting
- to conduct a feasibility study on the QdB system using quasi-static and dynamic models

1.4. Method and outline of thesis

This section describes the method applied and the structure of the thesis.

1.4.1. Method

A feasibility analysis aims to achieve a set of useful solutions for a design problem [1]. This thesis explorers the feasibility analysis. The method applied works with three research loops. At the end of each research loop, the feasibility of the QdB system is tested. The first research loop considers a quasi static analysis. A rough estimation can be done on the feasibility of the QdB system. The second research loop includes wave motions by applying the linear superposition method. It provides more details on the feasibility of the QdB system. The last research loop considers vessel motions by implementing Cummins' equation. Dynamics are included for the conceptual study. This provides an even better idea on the feasibility of the QdB system. The method described is part of design thinking. Divergence is used to develop the idea (second diamond (Figure 1.7): research loop 1 and 2) and convergence is used to deliver a useful detailed solution for the design problem (second diamond: research loop 3).

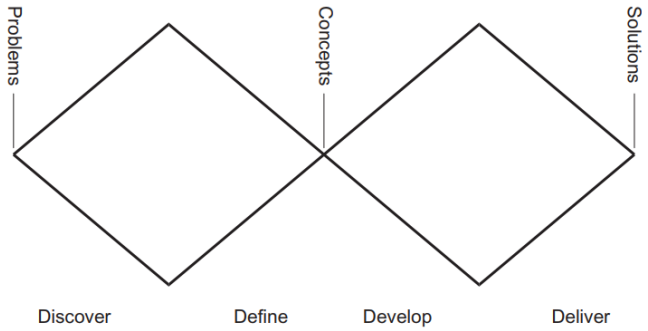

Figure 1.7: Double Diamonds [7]

1.4.2. Outline of thesis

The structure of the thesis is described in this subsection. An overview is given to show which research loops are covered in which chapters. The evolution of the model and the vessel motions included throughout the process are shown in this overview as well. DoF means Degrees of Freedom (Section 6.1).

Ch.	Title			
1	Introduction			
2	Literature study			
		Research loop	Model	Motions
3	The one tank model	-	Current QdB tank PS	-
4	QdB lifting challenges	-	-	-
5	A quasi static analysis	1	Requirements for lifting	heave
6	The superposition method	2	Wave excitation	heave + pitch
7	The Cummins equation	3	Wave excitation	6 DOF
8	Applying trim during fast lift	-	Wave excitation	6 DOF
9	Conclusions and recommendations			

1.5. Software

All models are generated using Python 3.7.3 with the interface Spyder. For hydrodynamic characteristics an existing model of AG's base case is used in ANSYS AQWA.

2

Literature study

To get a good understanding of what comes with ballasting for lifting, the 'full system' needs to be evaluated. For this chapter the 'full system' provides a broad understanding of a ballast system. This chapter describes the main topics found for the 'full system'.

QdB Systems: © P. S. Heerema et al in Ref [27] describe the use of a ballast system for stabilizing a crane vessel. All ballast water compartments above sea level are spaced along the circumference of the vessel. The main idea is to use ballast tanks above sea level on the corner columns to stabilize the vessel during heavy outboard loads by cranes. The ballast tanks below sea level are discharged by using pressurized air or the ballast of the tanks is pumped into the upper ballast compartments. The lower tanks are used to keep the vessel in horizontal position at rest. The whole system is controlled by means of a computer. The subaqueous hulls (Figure 2.1b: 1 and 2) have four columns at the end of them (Figure 2.1b: 3, 4, 5 and 6) and intermediate columns (Figure 2.1b: 7 and 8). The columns have a rectangular cross section. The corner columns have two chambers (Figure 2.1a: 9 and 10, 11 and 12). On of the two chambers is above water level (Figure 2.1a: 13). Before the operation, the upper chambers are full of water and the lower chambers are full of air. The upper part of the ballast system is for rising the vessel by discharging water in connection with the crane operation. The lower part of the ballast system causes a settlement of the vessel by letting water in, in connection with the crane operation. The control of water discharge is done by means of valves (Figure 2.1a: 16ab and 17ab). Vertical partitions divide the water ballast compartments into four sections (Figure 2.1b: 19 and 20). The outlet of these sections are indicated by 18a-d. Input data for the control of the system includes: the water level in the compartments, the crane vertical angle and the crane swing angle.

More specifically, © P. S. Heerema et al in Ref [26] also describe the use of ballast tanks for a semi - submersible crane vessel. The semi-submersible uses air chambers below sea level distributed along the circumferential outer zone of the vessel along the buoyancy hulls (Figure 2.2). At their lower side the air chambers

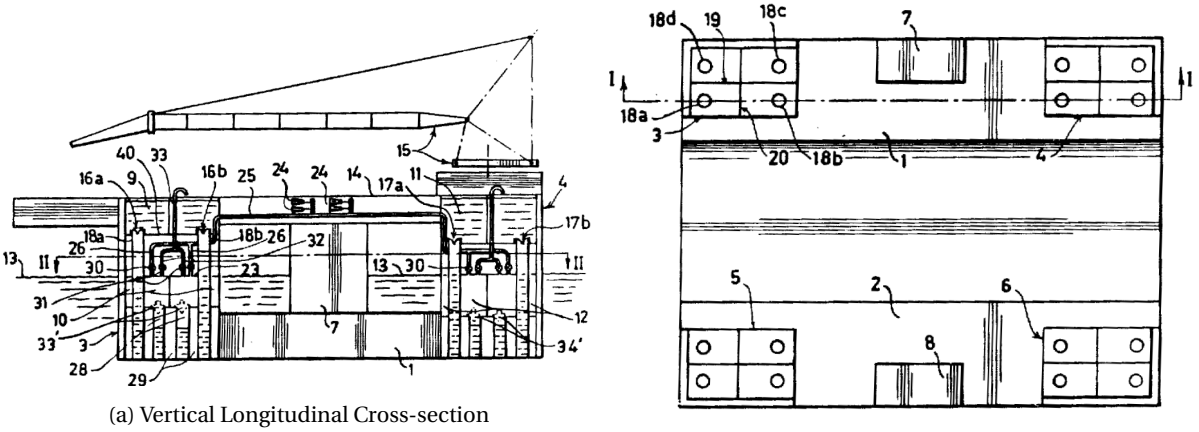

(a) Vertical Longitudinal Cross-section

(b) Horizontal Cross-section

Figure 2.1: Crane Vessel Using Ballast System [27]

are open to the surrounding water (Figure 2.2: 11 and 12) and at their upper part these chambers are connected to controlled air inlet and outlet (Figure 2.2: 24) conducts. The ceiling (Figure 2.2: 9 and 10) of the air chambers is below water level. An air compressor (Figure 2.2: 'c') forces air into the conduit, feeding the chambers 15 and 16 (Figure 2.2). A controlled air regulator valve (Figure 2.2: 13 and 14a), connecting to the compressed air volumes (Figure 2.2: 15 and 16), is opened and drives water out. Air could also be discharged from the compartments resulting in a raised water level. Vessel heave, vessel angles, the water level and the load's weight are the input to a computer to control the ballast tank flow.

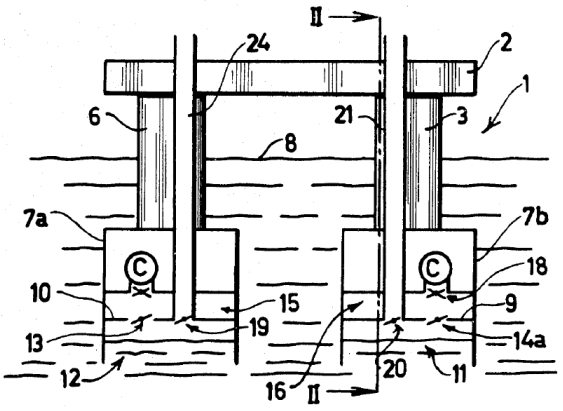

Figure 2.2: Semi-submersible with Ballast Tanks, Cross-section [26]

Submarines also use air under pressure to release ballast water very quickly. The paper [29] by R. Font et al describes a study on tank blowing and venting of manned submarines. This study can be applied to submarines and other marine systems using ballast tanks. R. Font and J. García-Peláez wrote another paper [30] on the hovering system based on the blowing and venting of ballast tanks. Mass, weight, moments- and products of inertia and the COG are expressed as a function of the amount of water in the tanks. The buoyancy is expressed as a function of the water depth. Controlling the hovering of the submarine can be done with a sliding control. T. I. Fossen and B. A. Foss published a paper [33] on the sliding control of MIMO Nonlinear Systems. MIMO is an abbreviation for Multivariable Input - Multivariable Output. Sliding control is applied in the control of underwater vehicle since they face highly nonlinear and time-varying parameters. Since motion control will not be implemented in the QdB system, the detail of controlling described in this paper is outside of the current thesis' scope.

Vessel Loading: The paper [13] written by H. Dankowski and H. Hatecke considers a stability evaluation of a semi-submersible (semi-sub) by a progressive flooding simulation tool. A numerical progressive flooding simulation method is introduced that is modified to simulate in time-domain. This paper is useful for the filling and the discharging of ballast tanks as filling is described in much detail. When discharging the ballast tanks, the water level in the ballast tanks varies. This introduces loadings, depending on the discharge time of the tank. D. Zhao et al wrote a paper [10] on nonlinear sloshing in rectangular tanks under forced excitation. The applied numerical code is based on potential flow and investigates the nonlinear sloshing in rectangular Liquefied Natural Gas (LNG) tanks. Both internal free surface elevation as sloshing loads can be obtained in time- and frequency domain. It has shown that an artificial damping model, introducing viscous effects, has the best applicability for simulating sloshing under different fill levels and excitations. Since the ballast tanks are expected to empty quickly, the sloshing effect may be neglected. For fast discharging ballast tanks, the vessel is expected to reduce her draught quickly. This could result into impact loading. "The structural behavior of ship's shell structures due to impact loading" is written by H. K. Lim and J. Lee [14]. The paper is written for the collision between ships or between a ship and an offshore platform. The amount of detail on dynamic flow stresses and dynamic hardening equations is assumed to be too much.

Submerging- and Float-over Operations: X. Wang and W. J. Ko studied the submerging operation design for heavy-lift barges based on a real case analysis [38]. For cargo loading and offloading, the vessel's main deck may need to be submerged to obtain a certain draught below sea level by flooding the vessel's ballast tanks. A few unsuccessful submerging operations are listed: Mighty Servant 3 (December 2006, semi-submersible, sank), POSH Mogami (July 2014, semi-submersible, sank), Dry Dock #3 (March 2012, floating dock, capsized). For numerical flooding simulations two categories are named: Bernoulli's equation and computational fluid dynamics (CFD). Of these simulation methods CFD is said to be not feasible for practical engineering usage yet. The chosen trial is simulated and the simulation is validated by matching the crews' descriptions and

photos. An analysis is done and a new flooding sequence is designed. The most interesting notion is that the submerging operation may start with flooding center tanks before side tanks. The side tanks can then be used for adjusting trim and heel at a later stage during the operation. The submerging method can be reversed to a float-over operation. During a float-over installation of an offshore platform's topside the topside is transported on a vessel at a certain draught. The draught is small enough for the vessel to float over the substructure that is already installed. The vessel can then increase it's draught to be able to install the topside on the substructure. Y. Ma et al wrote a paper on a numerical simulation of float-over installation for offshore platforms [39]. The hydrodynamic performance of a T-barge is described in frequency domain and the coupled motions are described in time-domain. The barge and topside interact through leg mating units and deck support units. The floating body motion equation in time domain (Cummins) is given. Since float-over installation is the reverse of the lifting operation of AG (float-over decommissioning), this paper is very useful for future numeric simulations included in the current master thesis.

Numerical Simulations: Since ballast water discharge has a direct influence on AG's draft, a time-domain simulation can be useful. Using the Cummins Equation provides the equations of motion with the addition of the convolution integrals over the past history of the velocity [8]. The coefficients are independent of frequency; this gives access to the equations of motion in time-domain (Equation 2.1)[6]

$$(M + A_\infty) \cdot \ddot{x}(t) + \int_0^t K(t-\tau) \cdot \dot{x}(t) d\tau + C \cdot x(t) = f_e(t) \tag{2.1}$$

with: x = array of DOFs (degrees of freedom), M = inertia matrix, A_∞ = added mass for the frequency going to infinity, K = transfer function, C = hydrostatic matrix and f_e = external forces. To compute the radiation terms, the integral, in Cummin's equation three methods are described by J. A. Armesto, R. Guanche, F. Jesus, A. Iturrioz and I. J. Losada[17]. The methods include: direct computation of the convolution integral (IRF method), an approximation by state space and an approximation of the impulse response function by Prony's coefficients. The author recommends the use of the IRF method and describes the steps that need to be taken. Numerical computations come along with required verification methods. C. J. Roy and W. L. Oberkampf wrote a paper on verification, validation and uncertainty quantification in scientific computing [5]. Uncertainties are characterized as 'aleatory' (characterized via a probability density distribution) and 'epistemic' (uncertainty due to lack of knowledge). The current master thesis will need a form of verification (characterizing numerical approximation errors associated with a simulation) or validation (showing the model accuracy by comparing simulation results with experimental measurements) when going through the research loops.

Detailed Design subjects: Maintenance logging and ballast water management would be of interest for a detailed design of the QdB system. This thesis does not provide a detailed design. For background information, some details are shared in this paragraph. *Maintenance logging:* The simulation of the QdB system will be tested for design requirements. These design requirements could be partly based on maintenance logging since maintenance logging is used to find the failure modes of a system as written by A.J. Mokashi et al in their paper 'A Study of Reliability-centred Maintenance in Maritime Operations'[2]. *Ballast Water Management:* Steel-hulled vessels are stabilized using ballast water. For safe and efficient modern shipping operations, ballast water is therefore essential. Marine species are carried in ship's ballast water, posing serious health, economic and ecological problems. The species that survive the transfer may reproduce in the host environment, becoming an invasive species. To minimize the effects, the 'International Convention and Management of Ships' Ballast water and Sediments' is adopted [16]. Guidelines are available. Since the QdB system will be (de-)ballasting in the same place, species will not be transported to another environment by means of ballast water directly. The empty tanks could still carry aquatic species. Therefore, the tanks should be kept clean.

The literature study provides a broad understanding on the topic, setting a foundation for the research that will be conducted according to the method shown in subsection 1.4.1.

3

The one tank model

Emptying out a tank aboard AG results in a change of draught for AG. The flow of water changes its velocity over time due to, for instance, the decreasing height of water in the tank. Since the flow has a direct consequence for the change in draught of AG, the QdB feasibility study starts by building a one-tank model. The model considers a singular tank. The results of the singular tank simulation are compared to test data of emptying a QdB tank of PS. This validates the one-tank model.

3.1. Tank configuration and position

Pioneering Spirit has four QdB tanks. The specifications of the four tanks together are described in subsection 1.1.3. For this section, the focus is on tank 13 and 14 of which test results are available. These tanks are located at the bow. The configuration of these tanks is the same. The cross sectional area of the tank varies over the height as shown in Figure 3.1. Figure 3.2 is an artistic impression of the position of the tank in the one tank model and the water heights from reference (h = 0) are shown. The tank is positioned in such a way that only vessel heave motions (Section 6.1) are allowed for.

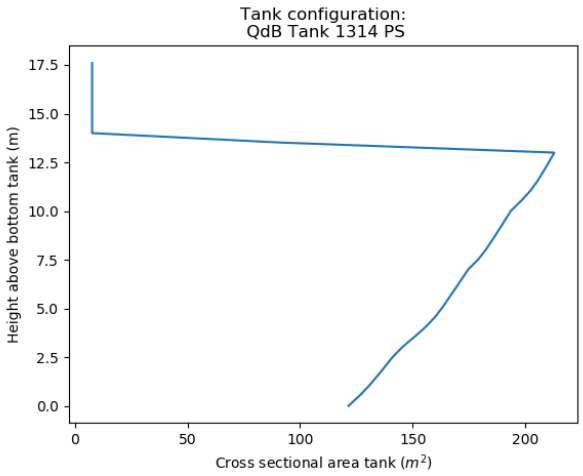

Figure 3.1: One Tank Model – Configuration Tank

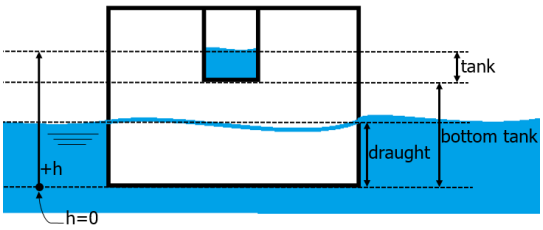

Figure 3.2: overview heights from reference

3.2. Mathematical model

Describing the problem of emptying a tank in a mathematical manner starts with a changing velocity over time. To derive the formulation of the changing velocity over time, energy in- and outputs to the water flow need to be considered. From this formulation a changing flow over time can be derived. The flow leads to a changing water height in the tank as a function of time. Since the volume in the tank is known as a function of height, the changing volume in the tank over time can be plotted. This plot is compared to the data received as test results.

A tank that empties by means of gravity has a pressure difference as an input to the system. Friction is the component that reduces the total amount of energy. The equations that are fundamental for the changing flow over time are shown in Equation 3.1 – 3.5.

$$\frac{dv(t)}{dt} = \frac{g \cdot (h_{tank}(t) - h_{level}(t))}{l_{pipe}} - f_D(t) \cdot \frac{1}{2} \cdot \frac{v(t)^2}{D_{outlet}} \qquad [\frac{m}{s^2}] \quad * \quad ** \tag{3.1}$$

$$A(t) = \frac{g \cdot (h_{tank}(t) - h_{level}(t))}{l_{pipe}}$$

$$B(t) = f_D(t) \cdot \frac{1}{2} \cdot \frac{v(t)^2}{D_{outlet}}$$

$$\frac{1}{\sqrt{f_D(t)}} = -2.0 \cdot log\left(\frac{\frac{\epsilon}{D_{outlet}}}{3.7} + \frac{2.51}{Re(t) \cdot \frac{1}{\sqrt{f_D(t)}}}\right) \quad (turbulent flow) \qquad [-] \quad ** \tag{3.2}$$

$$f_D(t) = \frac{64}{Re(t)} \quad (laminar flow, \quad Re(t) \leq 2000) \qquad [-] \quad ** \tag{3.3}$$

$$Re(t) = \frac{v(t) \cdot D_{outlet} \cdot \rho_{sea}}{\mu} \qquad [-] \quad ** \tag{3.4}$$

$$\frac{dQ(t)}{dt} = \int \left(\frac{dv(t)}{dt}\right) dA$$

$$= \frac{A_{outlet} \cdot g \cdot (h_{tank}(t) - h_{level}(t))}{l_{pipe}} - f_D(t) \cdot \frac{A_{outlet}}{2} \cdot \frac{v(t)^2}{D_{outlet}} \qquad [\frac{m^3}{s^2}] \tag{3.5}$$

* = [4] ** = [36]

Equation 3.1 shows the changing velocity over time. Part 'A' shows the pressure difference for which the height difference exists out of the tank water height + the height of the bottom of the tank - the water level (Figure 3.2). A change in draught causes this water level to be either equal to the draught itself or the height of the bottom of the tank. Part 'B' considers friction over the fall pipe. This is estimated by applying Colebrook's friction equation (Equation 3.2) or the laminar flow approximation (Equation 3.3), depending on the Reynolds number (Equation 3.4) (Figure 3.4). The roughness (ϵ) of the pipe's wall, the outlet diameter (D_{outlet}), the outlet velocity (v) and the water's density (ρ_{sea}) and viscosity (μ) are taken into account. Part 'A' and part 'B' are shown as function of time in Figure 3.3. Subtracting B from A results in a reduction of the flow. The changing flow over time (Equation 3.5) equals the changing velocity over time integrated over the cross sectional area (A_{outlet}). A list of variables is given on the next page.

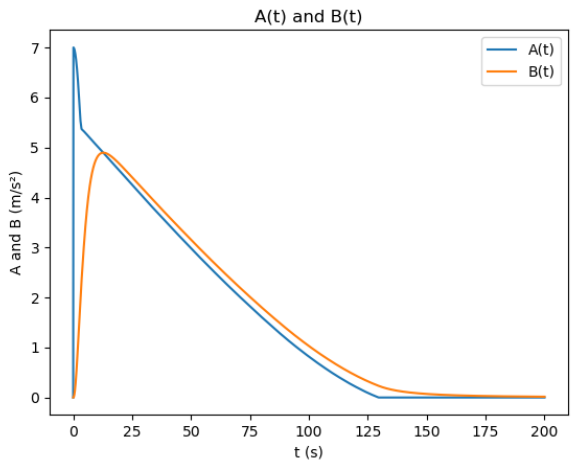

Figure 3.3: A and B from Equation 3.1

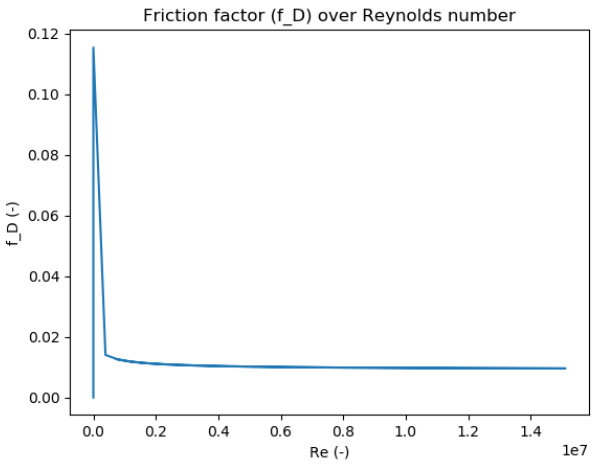

Figure 3.4: friction factor (f_D) for Reynolds number

A_{outlet} = outlet cross sectional area $[m^2]$
D_{outlet} = outlet diameter $[m]$
ΔV = change in tank volume = $V[t] - V[t-1]$ $[m^3]$
f_D = Moody friction factor $[-]$
g = gravitational constant = 9.81 $[\frac{m}{s^2}]$
$h_{bottomtank}$ = water height from keel to bottom of the tank = 16.4 [32] $[m]$
$h_{draught}$ = water height from keel to mean water level $[m]$
$h_{level} = \begin{cases} h_{bottomtank} & \text{when } h_{draught}(t) < h_{bottomtank} \\ h_{draught}(t) & \text{when } h_{draught}(t) \geq h_{bottomtank} \end{cases}$ $[m]$
h_{tank} = water height from bottom tank to water height in tank $[m]$
l_{pipe} = length of the fall pipe [32] $[m]$
PS_A = waterplane area of PS $[m^2]$
Q = flow $[\frac{m^3}{s}]$
Re = Reynolds number $[-]$
v = outlet velocity $[\frac{m}{s}]$
$\epsilon = roughness$ = 0.05 [36] $[mm]$
$\mu = viscosity$ = $1.07 \cdot 10^{-3}$ [37] $[\frac{kg}{m \cdot s}]$

3.3. Numerical approximation

When moving from a mathematical- to a numerical description, the changing flow over time is used for each time step (Equation 3.6). The volume as function of time (Equation 3.9) uses this flow approximation to find a volume reduction as function of time. The volume approximation is used to estimate the water height in the tank for a given water height to volume relation (Equation 3.7 and 3.8). Apart from the tank water height, the changing draught of the vessel is also an output. The changing draught is estimated by using the volume approximation and the water plane area of PS (Equation 3.10).

$$Q(t) = Q(t-1) + dt \cdot \frac{dQ(t)}{dt} \quad \text{(for Eq. 3.5)} \qquad [\frac{m^3}{s}] \tag{3.6}$$

$$h_{tank}(t) = h_{tank}(t-1) + \Delta h_{tank} \qquad [m] \tag{3.7}$$

$$\Delta h_{tank} = h_{tank}(\Delta V(t)) \qquad [m] \tag{3.8}$$

$$V(t) = V(t-1) - dt \cdot Q(t) \qquad [m^3] \tag{3.9}$$

$$h_{draught}(t) = h_{draught}(t-1) + \frac{\Delta V(t)}{PS_A} \qquad [m] \tag{3.10}$$

3.3.1. Extra frictional coefficient

The factors of transitional resistance (tank to pipe) and valve friction have not been taken into account yet due to time dependence. Since both factors would apply to the outlet, the cross sectional area of the outlet has been multiplied by a factor (Equation 3.11). This factor equals $\frac{2}{23}$. The factor has been based on matching the test data provided. For transitional resistance the factor would drop as the diameter increases. If the outlet changes from a butterfly valve to another type, the factor would change as well. Since the factor has been obtained by comparing to one set of test data only, the advice is to keep the coefficient a constant value. The coefficient is said to be of high uncertainty.

$$A_{outlet_{new}} = C_{friction}(\text{valve, streamlines}) \cdot A_{outlet_{old}} \tag{3.11}$$
$$A_{outlet_{new}} = \frac{2}{23} \cdot A_{outlet_{old}}$$

3.4. Convergence study

Figure 3.5 and Figure 3.6 show that for a decreasing time step the plots converge. The difference between the 0.1 and 0.01 seconds plots is small. An integral considering the volume over time for both time steps provides a difference of 0.059%. The plot can be said to have converged. Since it takes less time to plot for a bigger time step, a 0.1 second time step will be applied. The overlap with the volume from data also shows a validation. This validation is evaluated in the next section.

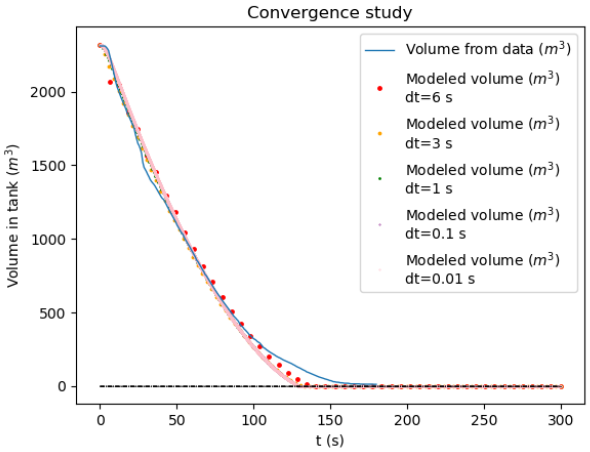

Figure 3.5: Convergence Study

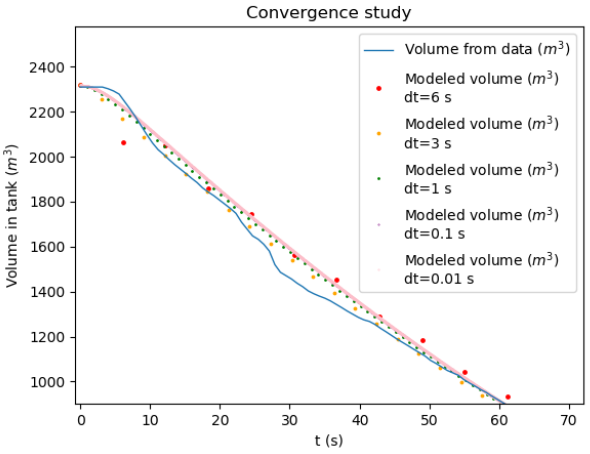

Figure 3.6: Convergence Study, details

3.5. Results and validation

Figure 3.7 shows the results of the one tank model using a singular tank with the dimensions of the QdB tank 13 and 14 of PS and the vessel dimensions of PS. The volume plotted in the upper half of Figure 3.7 results from Equation 3.9. The beginning of the height plotted shows a steep reduction. This is caused by the small cross sectional area as shown in Figure 3.1. Using the factor of $\frac{2}{23}$ a clear overlap is visible.

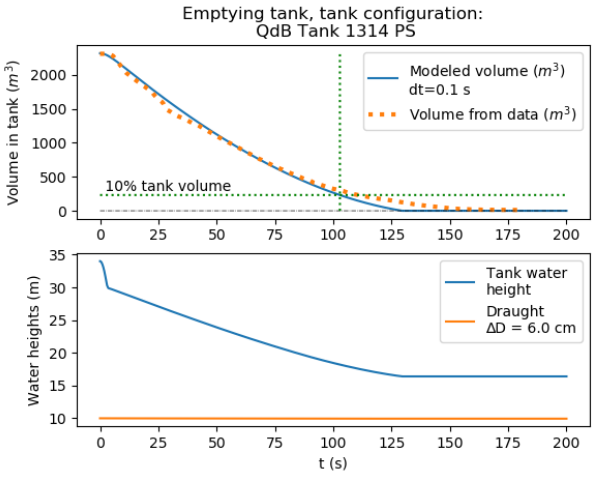

Figure 3.7: Volume and Water Height over Time

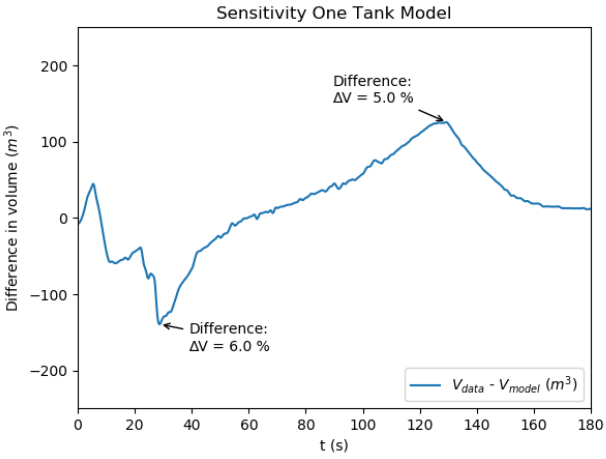

Figure 3.8: Sensitivity One Tank Model

The biggest differences between the modeled volume and the test data is shown for roughly 30 and 130 seconds in Figure 3.8. 6% of the full tank's volume is emptied out more for the data when comparing it to the modeled volume for the 30 second case. Since this part of the test data does not show a smooth trend, the difference could be caused by measurement errors for the test data. Therefore, the difference of 6% will not be studied any further. The 130 second case shows that 5% of the full tank's volume is emptied out more for the model when comparing it to the test data. Since this value occurs after less than 10% is left of the full tank's volume, non-linearities are expected to cause this part of the graph to empty out slower than the model. The non-linearities could be a direct consequence of a changing flow line curve when nearly emptying out the tank. This will not be included in the model since 5% is only a small percentage of the full tank's capacity. It can therefore be said that this difference is outside the current study's scope.

Given the acceptable difference of 5% between the modeled volume and the volume from test data, the model can be said to be validated. This model can be applied for further development.

4

QdB lifting challenges

Several challenges need to be faced when using QdB tanks to lift a topside. Five challenges are covered in this chapter, including: the airgap above Mean Sea Level (MSL), the pressure difference for emptying the tanks, the required volume stored in the tanks, the lifting phases applied and the position of the tanks. After elaborating on the challenges, the design requirements for the QdB system are shown. As the elaboration on the challenges explains the lifting conditions, the design requirements are the foundation for the quasi static analysis.

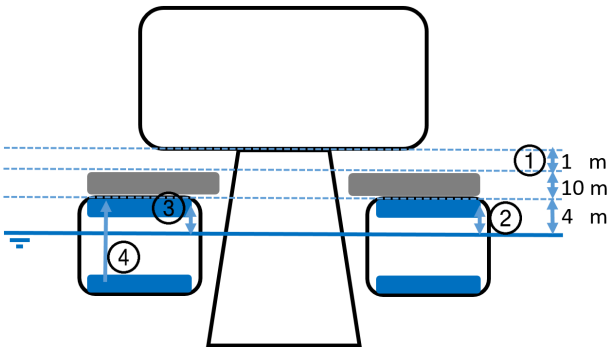

Figure 4.1: Challenges Feasibility

4.1. Airgap

The full airgap between MSL and the topside is 15 meters (subsection 1.1.4). Since beams will be used to lift the topside, the beam height needs to be subtracted from this gap. Only five meters remain as shown in Figure 4.1. The challenge is to combine keeping enough clearance from the topside to prevent early rebouncing (Figure 4.1, (1)) and remaining at such a freeboard that the pressure difference is as big as possible (Figure 4.1, (2)). The clearance from the topside has to be one meter (subsection 4.5: heave motion and safety factor), which provides a freeboard of four meters.

4.2. Pressure difference and required volume

For an airgap of one meter above AG's beams, there are only four meters left to create a pressure difference. This pressure difference is crucial to empty out the tank as quickly as possible. The bigger the pressure difference, the faster the tank would empty. The required time for emptying the tank needs to be in accordance with the peak period of 8 seconds as shown in section 4.5. Since AG is moving in upward direction when emptying her tanks, the height of the tank can be more than the available freeboard. The challenge is to see whether or not the tank's height in combination with the available area suits the volume to overcome the remaining airgap (Figure 1.6, (1)), to lift the topside of 72,000 tons (subsection 1.1.4) (Figure 1.6, (2)) and to create sufficient clearance to prevent rebounce of the substructure (Figure 1.6, (3)) within the time limit set by the peak period. The required volume is indicated as (3) in Figure 4.1.

4.3. Lifting phases

Lifting is done by applying lifting phases (subsection 1.1.3). When considering the lifting strategy for AG, there is a difference between lifting in one go and lifting using the lifting phases. The challenge for lifting in one go is that there will be no time to refill the tank. The volume contained in the tank has to be big enough to cover the required volume. If one lifts using the phases pretension (Figure 1.6, (2)) and fast lift (Figure 1.6, (3)), there will be time during the pretension phase to refill the tank as shown in Figure 4.1 as (4). The challenge is to see what the time frame would be to refill the tank considering the peak period of 8 seconds (subsection 4.5) and to see if this time frame is enough to fill up the tank with a big enough volume to continue to the next phase: fast lift. The quasi static analysis first addresses lifting in one go. If this is possible, refilling will not be studied.

4.4. Tank positions

When considering separate tanks, the position of these tanks in combination with the volume they hold can be seen as a challenge. Using an even number of tanks allows for a symmetric build up of AG's mass. The build up of AG's mass results in limitations considering the longitudinal vertical bending moment for instance. Furthermore, if a valve fails, the planned out build up could show a first impression on the vessel's response. The position of the tanks and the fail safety of the system should be studied for a detailed design case of the QdB system. This thesis does not provide the detailed design case.

4.5. Design requirements

AG has a response to a number of sea state variables. Since the topsides are expected to be decommissioned in the North Sea, a JONSWAP spectrum is chosen. The significant wave height (H_s), the peak period (T_p), the heave amplitude ($\zeta_{a,heave}$), the castellation and the safety margin are given an initial value. The list of design requirements presented in this section is based on Allseas' employees' expertise and the literature study. Section 7.4 shows a sensitivity analysis on the sea state variables. The requirements read as follows:

- Valve-related maintenance has been the most common corrective maintenance for the PS' QdB system. Ensure a fail safe QdB system.
- Create 1.5 meter clearance to avoid rebounce of the substructure after lifting the topside. The amount of clearance is based on:
  - The sea state: JONSWAP (head waves) H_s = 2.5 m, T_p = 8 s and $\zeta_{a,heave}$ = 0.5 m
  - Castellation of the substructure (Figure 4.2): 0.5 m
  - Safety margin: 0.5 m

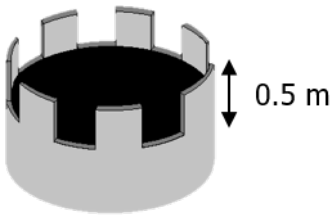

Figure 4.2: Castellation at the upper part of the cut in jacket leg

- Pretensioning needs to be done within 1.5 T_p
- Maintain a heeling angle of roughly 0°.
- The TLS (Topside Lift System) is able to withstand a trim of 1.5 m per AG's length. The maximum trim is 1.5 meters.
- Keep the tanks clean from aquatic species according to the guidelines set by IMO.

4.6. Chapter review

When using QdB tanks to lift a topside several challenges need to be faced. The airgap above the lifting beams of one meter to prevent early rebouncing allows for only four meters freeboard to create a pressure difference for emptying out the QdB tanks. Since AG moves upwards when emptying out her tanks, the height of the tank can be more than four meters. The challenge is to store enough water to reduce the draught with one meter, to lift the topside of 72,000 tons and to create 1.5 meter clearance to prevent rebounce of the substructure after lifting. This has to be done in accordance with the peak period of eight seconds. When considering lifting phases, the topside can be lifted in one go or by refilling the tanks. The challenge for lifting in one go is to see if all water could fit the volume available at AG. The quasi static analysis first considers lifting in one go. If this is possible, refilling will not be studied. It is recommended to study the tanks' positions considering bending moments and fail safety for a detailed design case of the QdB system.

5

A quasi static analysis

A quasi static analysis is conducted to get a first impression on what the volume of water would be to lift the topside and how many valves are required to lift the topside within the limited time. The quasi static analysis includes the main dimensions of AG and a singular tank. This tank contains a sufficient volume of sea water to be able to lift a topside and to create enough clearance from the jacket. The one tank model of chapter 3 is applied with a different volume to height relation. The tank is positioned in such a way to allow for heave motions only. By including only heave motions, the model is kept as simple as possible for this first estimation.

5.1. Dimensions

For the feasibility study a rectangular tank of 35049 x 6.5 (A x h) m^3 is chosen. The cross sectional area is fictitious and is chosen to give a quick estimation on whether the QdB system is feasible or not. The volume of $2.3 \cdot 10^5$ m^3, contained in the tank, shown on the vertical axis in Figure 5.1, is built up out of: a 1 meter gap, the topside of 72,000 ton with a safety factor of 1.1 and 1.5 meters extra clearance (subsection 4.5). By using the volume stated, a movement of 2.5 meters is achieved in ≈ 49 seconds (Figure 5.1). 60220 m^2 is the waterplane area of AG. For the movement of 2.5 meters, 500 valves (D = 2.2 m) with a total cross sectional area of roughly 1900 m^2 are applied to the tank. The tank area versus the waterplane area of AG is 58%.

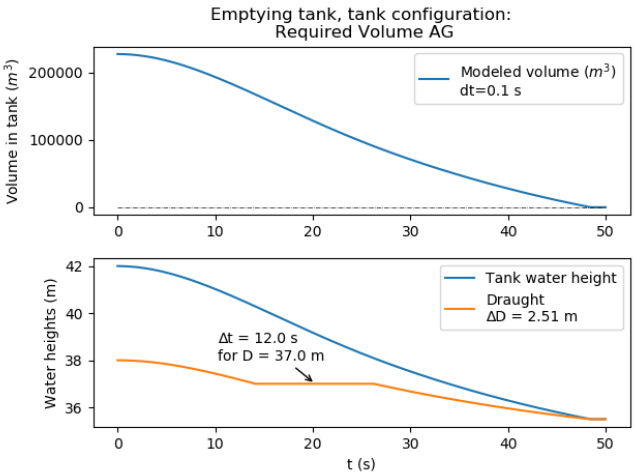

Figure 5.1: Feasibility Study AG

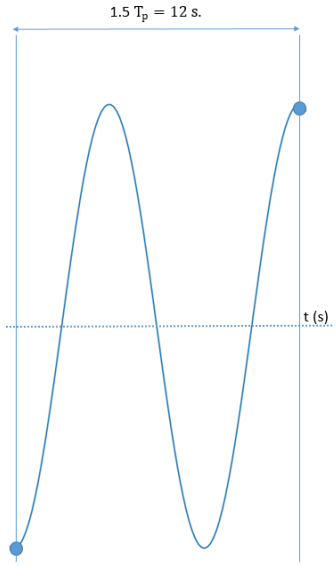

Figure 5.2: Proposed time taken: 1.5 T_p

5.2. Results review – quasi statics

The gap of one meter together with the lift of the 72,000 tons topside and the 1.5 meter extra clearance are covered using only 6.5 meters of tank height and $2.3 \cdot 10^5 m^3$. The required amount of valves (500) leads to a pretension phase. Pretensioning is done within 1.5 peak period. $\Delta t = 1.5 \cdot T_p = 12$ seconds (Figure 5.1). This is also shown in Figure 5.2 giving an initial indication on when to start pretensioning considering waves. The draught of 37 meters is constant for 12 seconds (Figure 4.1). Due to the connection and pretensioning at this plateau, this is called the connection plateau. The area (A) of the tank fits the waterplane area of AG. Refilling during the pretension phase is not required. An advantage to this is that no extra internal pumping system is needed to transfer the volume of water to a higher level (Figure 4.1, number (4)). This means that no time needs to be included for this separate operation to be fulfilled. Another advantage to not refilling the tanks is that the whole volume of water would be positioned as close to the deck as possible. When transferring the load of the topside to AG, the tanks are being emptied out. This means that the COG with respect to AG's draught would stay in roughly the same place, which is favourable for AG's stability. A disadvantage to not refilling the tank is that once you start deballasting, there is no stop to the process. Since this research is meant to show an overall feasibility of the QdB system without going into details about the design of the system, the disadvantage is not taken into account. This means that the QdB concept shows to be feasible in a quasi static analysis although the amount of valves large.

5.3. Chapter review

A quasi static analysis shows a first indication on whether the system is feasible or not. A rough indication is given by showing how much water is needed, how many valves are used and how much time is needed to empty out the volume of water. The assumption is made that all external influences on the system are set to zero. The assumption is valid for a first indication and the system shows to be feasible. In reality waves will influence AG's motions. The next step is to include wave excitation in the model.

6

The superposition method

For a vessel as big as AG, the motions are assumed to be small during a lift. This is why an initial derivation of her motions in waves can be done through the linear superposition method. This chapter discusses the degrees of freedom of ships which lead to the equations of motion. The linear superposition method is introduced and the required time series' duration is derived by applying this method. The maximum heave amplitude is chosen based on a statistical analysis. This amplitude is applied to the connection plateau to see what the effect would be. At the end of the chapter the effect at the connection plateau translates into a conclusion on the QdB system's feasibility.

6.1. Degrees of freedom

Without mooring, every vessel has six degrees of freedom (DoF). The motions $[x, y, z, \phi, \theta, \psi]$ (Figure 6.1) represent surge, sway, heave, roll, pitch and yaw. Since the angles of rotation (ϕ, θ, ψ) are assumed to be small, the motions of AG can be approximated linearly. The linear approximation of AG's motions in a singular point is shown in Equation 6.1 [20].

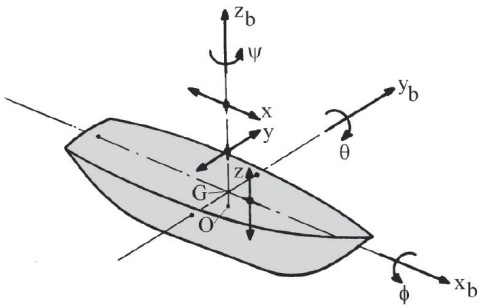

Figure 6.1: Degrees of Freedom Ship [18]

$$
\begin{aligned}
x_p &= x - y_b\psi + z_b\theta \\
y_p &= y + x_b\psi - z_b\phi \\
z_p &= z - x_b\theta + y_b\phi
\end{aligned} \tag{6.1}
$$

6.2. Equations of motion

The six DoF are combined in an equation of motion (Equation 6.2). The mass (m), added mass (a) and inertia factor (I_{zz}) are shown in the first term. The damping coefficient (b) is followed by the restoring spring coefficient (c). Head waves are assumed, giving an initial loading condition for lifting with two bows. Since the underwater profile of AG is symmetric with her COG at y = 0 meters, the heeling angle (ϕ) is zero degrees. Surge is not included in this study since we are interested in the motions in z-direction. For the actual procedure, surge could be counteracted by applying dynamic positioning (DP), using thrusters to stay in place. This results in a two degrees of freedom study considering pitch and heave. For considering only heave and pitch motion the shortened version of Equation 6.2 is shown in Equation 6.3.

$$\begin{bmatrix} m+a_{11} & \dots & a_{16} \\ \vdots & \ddots & \vdots \\ a_{61} & \dots & I_{zz}+a_{66} \end{bmatrix} \cdot \begin{bmatrix} \ddot{x} \\ \ddot{y} \\ \ddot{z} \\ \ddot{\phi} \\ \ddot{\theta} \\ \ddot{\psi} \end{bmatrix} + \begin{bmatrix} b_{11} & \dots & b_{16} \\ \vdots & \ddots & \vdots \\ b_{61} & \dots & b_{66} \end{bmatrix} \cdot \begin{bmatrix} \dot{x} \\ \dot{y} \\ \dot{z} \\ \dot{\phi} \\ \dot{\theta} \\ \dot{\psi} \end{bmatrix} + \begin{bmatrix} c_{11} & \dots & c_{16} \\ \vdots & \ddots & \vdots \\ c_{61} & \dots & c_{66} \end{bmatrix} \cdot \begin{bmatrix} x \\ y \\ z \\ \phi \\ \theta \\ \psi \end{bmatrix} = \begin{bmatrix} F_x \\ F_y \\ F_z \\ M_x \\ M_y \\ M_z \end{bmatrix} \tag{6.2}$$

$$(m+a_{33}) \cdot \ddot{z} + a_{35} \cdot \ddot{\theta} + b_{33} \cdot \dot{z} + b_{35} \cdot \dot{\theta} + c_{33} \cdot z + c_{35} \cdot \theta = F_z + F_{topside} \tag{6.3}$$

F_z is the wave force. The wave force has a harmonic shape. The QdB plot (Figure 5.1) is generated in time domain and the wave induced vessel motions will have to be added this plot. This is the reason why the vessel motions are derived linearly in time domain using the superposition method. By doing so, an indication on the vessel motions of AG, when applying QdB, is provided.

6.3. Linear superposition

The time histories of vessel motions can be gained through the superposition principle. A number 'N' of frequency (ω_n) based waves, with wave amplitude (ζ_{a_n}), are added together as shown in Equation 6.4 [22]. This equation uses randomly chosen phase shifts (ϵ_n) of the wave between 0 and 2π. The spectral characteristics are included through Equation 6.5 [22] with a spectral density $S_\zeta(\omega_n)$ calculated using a JONSWAP spectrum. Vessel motions are derived using this wave motion, a transfer function $\frac{Z_{wa_n}}{\zeta_{a_n}}$ (RAO amplitude) and a phase shift $\epsilon_{Z_w\zeta_n}$ (RAO phase) as shown in Equation 6.6 [22]. The RAO data is calculated using the potential solver ANSYS AQWA and the base case design of *Amazing Grace* . The time history repeats itself after $\frac{2\pi}{\Delta\omega}$ seconds for a constant frequency interval $\Delta\omega$. [22]

$$\zeta(t) = \sum_{n=1}^{N} \zeta_{a_n} cos(\omega_n t + \epsilon_n) \tag{6.4}$$

$$\zeta_{a_n} = \sqrt{2 \cdot S_\zeta(\omega_n) \cdot \Delta\omega} \tag{6.5}$$

$$Z_w(t) = \sum_{n=1}^{N} \left(\frac{Z_{wa_n}}{\zeta_{a_n}} \right) \cdot \zeta_{a_n} cos(\omega_n t + \epsilon_n + \epsilon_{Z_w\zeta_n}) \tag{6.6}$$

6.4. Time series duration

A rule of thumb is to use 15-30 min of wave record time series [12]. To get a better understanding of the duration needed to have an accurate representation of the wave spectrum used, a statistical analysis is done. The standard deviation of the heave amplitude is used for this. For a converging standard deviation of the heave amplitude, no unforeseen motions are expected to be in the time series. Mathematically, the standard deviation (σ) of the heave amplitude and the maximum amplitude of the time series (ζ_{max}) are calculated using Equation 6.7 – 6.9 [21].

$$\sigma = \sqrt{\frac{1}{N-1} \sum_{n=1}^{N} \zeta_n^2} \tag{6.7}$$

$$\zeta_{a_{\frac{1}{3}}} = 2 \cdot \sigma \tag{6.8}$$

$$\zeta_{max} = \zeta_{a_{\frac{1}{3}}} \cdot 1.86 \tag{6.9}$$

Over a given time series, the maximum heave amplitude and σ should both converge to a single value according to the relation aforementioned. Numerically, the convergence study is performed by increasing the time span each time step for the calculation of both the maximum amplitude and the standard deviation of the heave amplitude time series. The outcomes of four time series runs are shown in Figure 6.2. Since the maximum heave amplitude is directly related to the randomized phase of the waves, the maximum heave amplitudes of the various time series do not necessarily converge. ζ_{max_1} (green) in Figure 6.2 shows the best match to the relation of Equations 6.7 - 6.9. The expected maximum heave amplitude, with a probability of $\frac{1}{1000}$, is calculated by using the converged standard deviation for Equation 6.8 and 6.9.

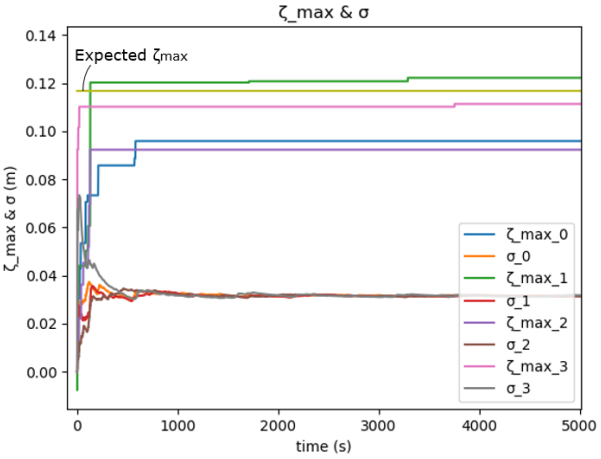

Figure 6.2: 4 time series - 100000s full run - ζ_{max} and σ

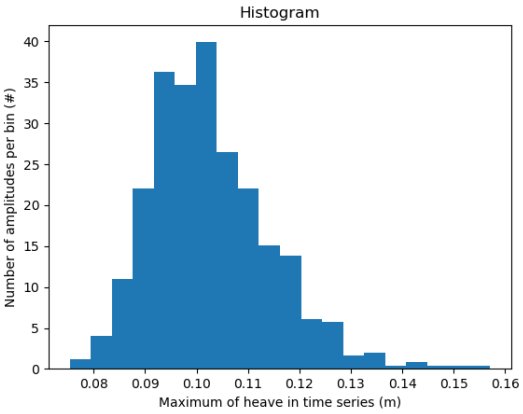

Figure 6.3: Probability of maximum heave amplitude

For a converged σ (Figure 6.2), the required time is set to 1200 seconds (= 20 min), meeting the 15 - 30 min rule of thumb. As the peaking of the time series for the maximum heave amplitude is unpredictable due to the randomized wave phases, ζ_{max} cannot be taken into account for estimating the time series' length.

6.5. Probability of occurrence

The connection plateau considers connecting and pretensioning till fast lift. Rebounce during pretensioning is unfavourable and therefore the connection plateau needs to be studied. For a heave amplitude at the connection plateau, a statistical analysis is done. The time span from the previous section is used to generate 600 time series. The maximum heave amplitude of every time series is found to define a probability as shown in the histogram (Figure 6.3). The distribution has a Rayleigh characteristic with a most common maximum amplitude just above 0.1 meters. A heave amplitude of 0.106 m is applied to the connection plateau because of the high probability.

This high probability can be linked to wave elevation predictions through marine radar imaging [24]. This technology is still under continuous development and accuracy is continuously improved. The accuracy of a marine radar for sea surface recording has to be indicated before using it in marine operations [11]. Since AG will be built in the far future, it is assumed that there is enough time to implement the marine radar imaging accurately for predicting the significant wave height, which leads to AG's heave amplitude. This is why the most probable heave amplitude provides a good estimation for the current master thesis' research.

6.6. Connection

The full heaving motion is a combination of heave and pitch at the bow (Equation 6.1). This results in an amplitude of roughly 0.2 meters. When applying this motion to the connection plateau (plateau: Figure 5.1) with the actual heave amplitude at it's maximum as calculated in the previous section, an indication of AG's response is given in Figure 6.5.

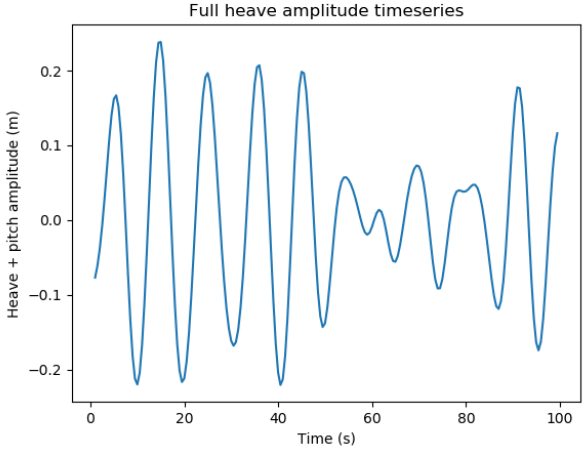

Figure 6.4: Heave + pitch

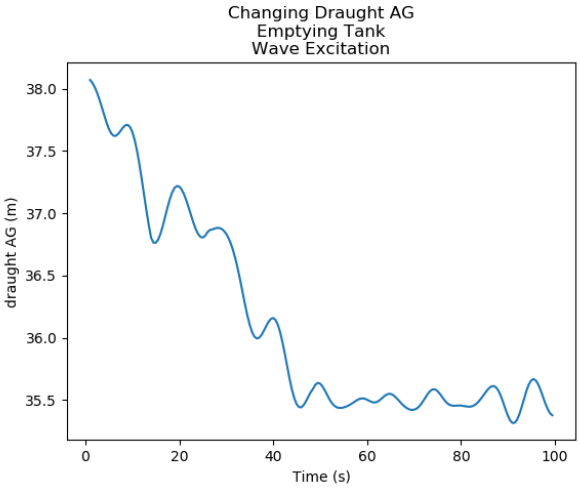

Figure 6.5: Changing draught with wave excitation

6.7. Chapter review

The linear superposition method is used to provide a first estimation on AG's motions in waves. The method is linear, which means that only small angled motions can be derived. The dimensions of AG and the full heave amplitude of roughly 0.2 meter combined result in small angled motions. The motions are calculated using RAOs. No mass, added mass, damping or stiffness of the vessel are included. Due to AG's inertia, AG would respond slower to deballasting than currently calculated through the linear superposition method. Since timing with respect to connecting AG to the topside is important, a more accurate dynamic model with respect to the previously mentioned coefficients of the equation of motion is required. A better understanding of QdB's feasibility, providing details on both connecting to the topside and rebounce of the jacket after lifting the topside, is needed.

7

The Cummins equation

To get a better estimation on the connection with the topside, a more accurate dynamic model needs to be generated including AG's mass, inertia, added mass, damping and stiffness. That is why the equation of motion is implemented through Cummins' equation providing AG's motions in time domain. By implementing the equation, excitational wave forces moving AG (diffraction forces) and wave forces produced by the movements of AG itself (radiation forces) can be accounted for. The latter is also known as the fluid memory effect [17]. Other external forces, such as mooring or QdB, can also be included in the equation. This chapter provides the mathematics, numerics and the verification of the implementation of the Cummins equation, a sensitivity analysis is done and the chapter ends with a conclusion on the feasibility of the QdB system.

7.1. Mathematical model

To compute AG's motions more accurately in time domain, Cummins' equation combines AG's mass matrix (M), the frequency dependent added mass matrix with the frequency going to infinite (A_∞), AG's stiffness matrix (C), the impulse response function (B(t - τ)) and external forces (Z(t)) in Equation 7.1 [8]. The external forces consider wave diffraction, wave radiation forces and the deballasting of the QdB system. The impulse response function is derived as radiation force in subsection 7.2.2.

$$(M + A_\infty) \cdot \ddot{z}(t) + \int_0^t B(t-\tau) \cdot \dot{z}(\tau) \cdot d\tau + C \cdot z(t) = Z(t) \tag{7.1}$$

$$\ddot{z}(t) = \frac{1}{(M + A_\infty)} \cdot \left(Z(t) - \int_0^\infty B(t-\tau) \cdot \dot{z}(\tau) \cdot d\tau - C \cdot z(t) \right) \tag{7.2}$$

$$\dot{z}(t) = \int_{t=0}^{t=t_{end}} \ddot{z}(t)\, dt \tag{7.3}$$

$$z(t) = \int_{t=0}^{t=t_{end}} \dot{z}(t)\, dt \tag{7.4}$$

7.1.1. Diffraction force

Wave forces that excite AG's motions are diffraction forces. Harmonics can be written in complex notation considering an imaginary and a real part [25]. The force RAO amplitude ($\frac{F_{a\omega}}{\zeta_{a\omega}}$) and the force RAO phase ($\epsilon_{F_\omega \zeta_\omega}$) are the foundation of the imaginary and real part of the diffraction force as shown in Equation 7.5 and 7.6 [25]. Summing for all frequencies provides a time series of the diffraction force as shown in Equation 7.7 and 7.8 [25]. ζ_a is the single wave amplitude derived from the JONSWAP wave spectrum. The spectrum applied focuses on a wave period in the range of 6 till 10 seconds; the chosen peak period of 8 seconds fits this range. ω is the set of frequencies belonging to these wave periods and ϵ is the wave phase which is randomly seeded between 0 and 2π. The final diffraction force is the sum of the imaginary and the real part as shown in Equation 7.9.

$$Im(\omega) = \frac{F_{a_\omega}}{\zeta_{a_\omega}} * cos(\epsilon_{F_\omega \zeta_\omega}) \qquad [\frac{N}{m}] \qquad (7.5)$$

$$Re(\omega) = \frac{F_{a_\omega}}{\zeta_{a_\omega}} * sin(\epsilon_{F_\omega \zeta_\omega}) \qquad [\frac{N}{m}] \qquad (7.6)$$

$$F_{Im}(t) = \sum_{min(\omega)}^{max(\omega)} \zeta_a \cdot sin(\omega t + \epsilon) * Im(\omega) \qquad [N] \qquad (7.7)$$

$$F_{Re}(t) = \sum_{min(\omega)}^{max(\omega)} \zeta_a \cdot cos(\omega t + \epsilon) * Re(\omega) \qquad [N] \qquad (7.8)$$

$$F_{diff}(t) = F_{Im}(t) + F_{Re}(t) \qquad [N] \qquad (7.9)$$

7.1.2. Radiation force

Forces generated by the moving body of AG are called radiation forces. An example of the radiation force induced by a rowing blade is shown in Figure 7.1. The mathematical derivation of the radiation force is shown in Equation 7.10 – 7.12 [19]. According to potential theory, the radiation potential ($\Phi_j(x,y,z,t)$), associated with the oscillation of a body in still water (the rowing blade for instance) is written in terms of 6 DoF (Equation 7.10) of which 'j' is a singular direction. The space and time dependent potential term $\Phi_j(x,y,z,t)$ is split into a space dependent potential term $\phi_j(x,y,z)$ and the oscillatory velocity $v_j(t)$. The normal velocity on the surface of the body is written in Equation 7.11. The radiation force as function of the space dependent potential can now be formulated as an integration over the submerged surface (dS) with an outward normal vector $\vec{n}$ (Equation 7.12). This force will be translated into a numeric approximation in subsection 7.2.2.

$$\begin{aligned} \Phi_r(x,y,z,t) &= \sum_{j=1}^{6} \Phi_j(x,y,z,t) \\ &= \sum_{j=1}^{6} \phi_j(x,y,z) \cdot v_j(t) \end{aligned} \qquad (7.10)$$

$$\begin{aligned} \frac{\delta \Phi_r}{\delta n} &= \frac{\delta}{\delta n} \sum_{j=1}^{6} \Phi_j \\ &= \sum_{j=1}^{6} \left\{ \frac{\delta \phi_j}{\delta n} \cdot v_j \right\} \end{aligned} \qquad (7.11)$$

$$\begin{aligned} \vec{F}_{rad} &= \rho \int_S \int \left(\frac{\delta \Phi_r}{\delta t} \right) \vec{n} \cdot dS \\ &= \rho \int_S \int \left(\frac{\delta}{\delta t} \sum_{j=1}^{6} \phi_j v_j \right) \vec{n} \cdot dS \end{aligned} \qquad (7.12)$$

Figure 7.1: Radiation force

7.1.3. QdB force

The force exerted by debalasting the QdB system (F_{QdB}) is applied at AG's COG (Figure 7.2). The difference in volume introduces a force as shown in Equation 7.13.

$$F_{QdB}(t) = \Delta V \cdot \rho_{sea} \cdot g \qquad [N] \qquad (7.13)$$

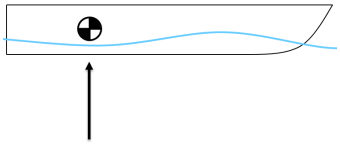

Figure 7.2: QdB force

7.2. Numerical approximation

The aforementioned mathematical model is approximated numerically [31]. A flowchart of the full calculation is given in Figure 7.3. The numerical description is provided in this section, starting with the acceleration to motion conversion. Equations 7.14 – 7.16 show the conversion from acceleration (a) to the motions of AG (u). v is the velocity and Δt is the time step. The forward Euler method is applied. This is common practice

for solving ordinary differential equations. The advantage of the Euler method is the simple implementation. A downside is the demand for small integration time steps causing a slow computation of the solution [34].

$$a(t+1) = \left[M + A_{inf}\right]^{-1} \cdot \left(F_{diff}(t) + F_{QdB}(t) + F_{rad}(t) - C \cdot u(t)\right) \quad [\frac{m}{s^2}] \quad (7.14)$$

$$v(t+1) = v(t) + \frac{1}{2} \cdot \Delta t \cdot \left(a(t) + a(t+1)\right) \quad [\frac{m}{s}] \quad (7.15)$$

$$u(t+1) = u(t) + \frac{1}{2} \cdot \Delta t \cdot \left(v(t) + v(t+1)\right) \quad [m] \quad (7.16)$$

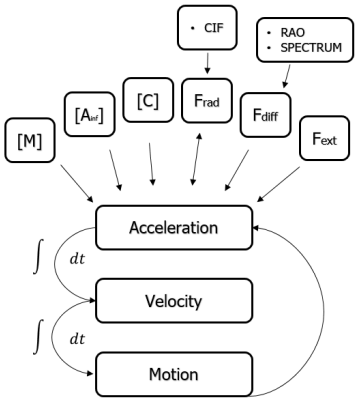

Figure 7.3: Cummins' flowchart

7.2.1. Diffraction force

For n number of frequencies, the diffraction force is approximated as shown in Equation 7.17 – 7.19. ζ_a is based on the JONSWAP spectrum. $Im(\omega_n)$ and $Re(\omega_n)$ are calculated as shown in Equation 7.5 and 7.6 respectively.

$$F_{Im}(t) = F_{Im}(\omega_{n-1}, t) + \zeta_a \cdot sin(\omega_n t + \epsilon_n) \cdot Im(\omega_n) \quad [N] \quad (7.17)$$

$$F_{Re}(t) = F_{Re}(\omega_{n-1}, t) + \zeta_a \cdot cos(\omega_n t + \epsilon_n) \cdot Re(\omega_n) \quad [N] \quad (7.18)$$

$$F_{diff}(t) = F_{Im}(t) + F_{Re}(t) \quad [N] \quad (7.19)$$

7.2.2. Radiation force

The radiation force is implemented using a time history. The convolution integral function (CIF) needs to be calculated over all frequencies (Equation 7.20). This can be done by applying the IRF method described by J.A. Armesto et al.[17]. The damping coefficient, $b(\omega)$, needs to be computed for all frequencies. This is done by using ANSYS AQWA. The interpolated [CIF], over a number of time steps in the interval [0,120], is exported from ANSYS AQWA. Together with the acceleration history, this results into the radiation force as shown in Equation 7.21. The acceleration history is directly linked to a time history. This time history is based on a memory time set as an input.

$$B(t) = \frac{2}{\pi} \int_0^\infty b(\omega) cos(\omega\tau) d\omega \quad (7.20)$$

$$F_{rad}(t) = acc_{history} * [CIF] \quad [N] \quad (7.21)$$

All numerical approximations are implemented. The verification of the implementation is given in the next section.

7.3. Verification of implementation

The first step in the verification of the implementation is to see which time step suits the model the best. A convergence study is conducted to see which time step is needed. The time step required is based on a set of 4 time series with different time steps. The difference between the areas under the graphs gets smaller for a smaller time step. A balance is found between accuracy and the time needed to run the simulation by not choosing the smallest time step. A conclusion on the time step needed is based on comparing the three hours maximum amplitudes for the two smallest time steps. If these values compare, the convergence study is closed. After the convergence study, a comparison is made between the frequency- and the time domain to verify the implementation of the Cummins equation (time domain). In frequency domain, ANSYS AQWA calculates AG's motions from which a motion report is produced. These motions are compared to the motions calculated in time domain using the Cummins equation implementation.

7.3.1. Convergence study

The heave motion at AG's COG for the QdB excitation in z-direction is computed for a set of four time steps (dt). Figure 7.4 shows that for a smaller time step, the solution converges and that for the bigger time steps the system gets unstable due to the summation of errors. The output for 0.01 and 0.04 dt show a similar converging behaviour. The standard deviation for 0.01 dt is 0.27 with a three hours maximum of 1.02 meter (Equation 6.9). The 0.04 dt has a standard deviation of 0.28 and a three hours maximum of 1.04 meter. 2 cm difference can be neglected for a vessel of AG's dimensions with a safety margin of half a meter. For dt = 0.04 seconds the model shows similar dynamic behaviour as for dt = 0.01 seconds. The time step of 0.04 seconds is used for further calculations.

Apart from showing the convergence analysis, Figure 7.4 also shows the first results of the implementation of Cummins' equation for H_s = 2.5 meters, T_p = 8 seconds and the QdB force at AG's COG. Heave at the bow is plotted for a time series of 1200 seconds from which 700 seconds are shown. At 26 seconds the fast lift starts which results in a total vertical movement of 1.5 meters. This is in accordance with the design requirements (section 4.5) for covering the heave amplitude, the safety margin and castellation. AG and the topside aboard act as a mass spring damper system being excited by the QdB force and the wave forces. The dampening is caused by radiation forces and the restoring spring coefficient of AG is the stiffness.

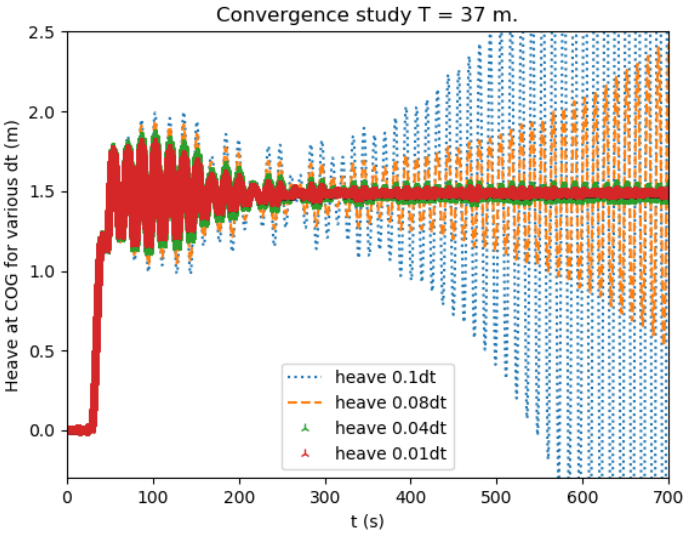

Figure 7.4: Convergence T = 17 m,
[0, 700] seconds of 1200 second time series

7.3.2. Time- versus frequency domain

Motion report data (Appendix B, frequency domain) provides a three hours maximum for motions, velocities and accelerations. The Cummins equation implementation is in time domain. Since the models are either computed in time- or frequency domain, one could compare their outcomes to see if they match. By comparing the outputs, the expectation of the response of the computation algorithm, set by the motion report, is checked for the Cummins equation implementation. If the outcomes are comparable it is demonstrated that the Cummins equation implementation is verified. The most probable three hours maximum of the various motions in time domain are calculated according to Equation 6.9. Except for the wave force, no additional external force is applied.

	Motion report		Cummins' implementation		
	3 hrs max amplitude	σ	3 hrs max amplitude	σ	
z	0.34	0.092	0.34	0.093	[m]
θ	0.056	0.015	0.0016	0.00044	[rad]

Table 7.1: Motion comparison, for T = 17m

AG is not moored in the model of the implementation of Cummins' equation. Therefore, surge, sway and yaw can not be compared to the values of the motion report. For head waves, roll is zero radians. The comparison for heave and pitch at the bow is shown in Table 7.1. As the σ values get close, the three hours maximum amplitudes are also in the same range.

The convergence study and the comparison between time- and frequency domain demonstrate that the implementation of the Cummins equation is verified.

7.4. Sensitivity analysis

When using the described model (Section 7.2), the design variables are assumed to be of a certain value. The significant wave height H_s was assumed to be 2.5 meters, the peak period T_p was set to be 8 seconds, the wave direction was assumed to be π radians (180 degrees) and the peak enhancement factor γ was set to be 3.3. For a change in draught the coefficients of Cummins' equation vary. These coefficients were assumed to be constant. The design variables as well as the design parameters are shown in Table 7.2.

Design parameters		Design variables		
COG	[m]	H_s	[m]	
ω	[rad/s]	T_p	[s]	Sea state
Δt	[s]	Wave direction	[rad]	
Time vector	[s]	γ	[-]	
Translation matrix	[-]			
Tank volume	$[m^3]$	$[M]$	[tons]	
Memory time	[s]	$[A_\infty]$	[tons]	Cummins'
$\Delta t_{memorytime}$	[s]	$[C]$	[N/m]	coefficients
$RAO_{force,amplitude}$	[N/m] [N m/rad]	CIF	$[Ns^2/m]$	
$RAO_{force,phase}$	[rad]			

Table 7.2: An overview of design parameters and -variables

From the list of design parameters, the translation matrix refers to the translation from COG to the position at the bow, the memory time is a value used for the radiation force and so is the time step for the memory time. One wants to know what the effect is on the motions of AG when changing the design variables. Therefore, this section shows a sensitivity analysis on the design variables. The sensitivity analysis is split into two main subjects: the sea state and Cummins' coefficients.

7.4.1. Sea state

For the analysis the heave motion at the bow is studied after the fast lift has been executed. When changing the sea state design variables, the system could experience a bigger excitation (Figure 7.4, ≈ 100 seconds). An example for a bigger excitation is when using a bigger value for the significant wave height. Because of the mass spring damper characterization, AG's bow is expected to move downward over a bigger distance when experiencing a bigger excitation. This could result into rebounce of the jacket after fast lift. Therefore, the minimum heave position after fast lift is studied in this sensitivity analysis. T_p is varied after which γ will be varied using a significant wave height in the range of 1.5 – 3.5 meters.

H_s = 1.5 m (Figure 7.7a and 7.7d): The heave positions for T_p = 6 and 8 seconds are both distributed neatly between 0.4 and 0.5 meters for all directions. For T_p = 9 seconds, the result has a different behaviour. This peak period shows that the wave direction has an influence on the minimum heave position. Up and till 60 degrees, the position is distributed between 0.3 and 0.4 meters. The biggest response is shown for 75 degrees waves.

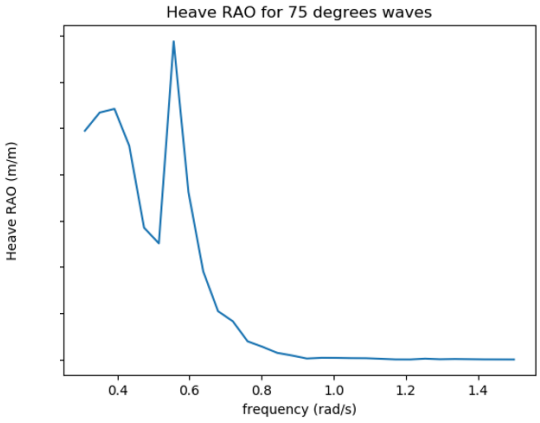

Figure 7.5: Heave RAO at bow 75 degrees waves, T = 17m

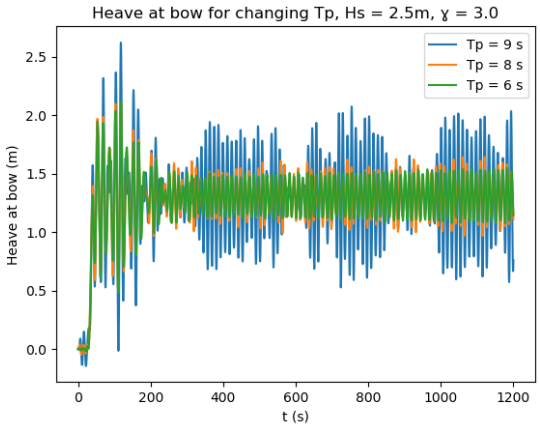

Figure 7.6: Heave at bow 75 degrees waves, T = 17m

The 75 degrees heave RAO at the bow is plotted in Figure 7.5. The peak of this RAO is found at 0.6 rad/s. For a peak period of 9 seconds: $\frac{2\pi}{9} = 0.7\frac{rad}{s}$. This does not correspond to the 0.6 rad/s. For an increasing peak period, the time series for heave are plotted in Figure 7.6. It is clear that for an increasing peak period, AG's response is bigger. This can be explained by the fact that for a bigger peak period, one gets closer to the frequency of 0.6 seconds in Figure 7.5. For 105 degrees and above, the minimum heave position is roughly 0.5 meter and above (Figure 7.7a); this means that the response is minimal. When looking at the variation for γ at 1.5 meters H_s, a similar behaviour occurs (Figure 7.7d). For 105 degrees and above, the variation in γ does not influence the response of AG anymore. The minimum heave positions are of roughly the same value given its variation in γ. The minimum heave position is influenced by the value of γ for the wave directions below 105 degrees. For a higher γ, more energy is contained in the spectrum, so a bigger response is expected. A higher value for γ shows a lower minimum heave position, which is a bigger response.

H_s **= 2.5 m (Figure 7.7b and 7.7e)**: The behaviour for the three T_p values is very similar to H_s = 1.5 meters. For T_p = 6 and 8 seconds, the heave positions are of approximately the same values as the previous data set. Only T_p = 9 seconds, shows a big difference. As expected, the minimum positions decrease for an increasing significant wave height when looking at the wave directions up and till 105 degrees. For wave directions above 105 degrees, the minimum heave positions do not show much of a difference when comparing it to the 1.5 meter significant wave height data set. For the variation of γ only small changes occur of which the biggest changes appear up and till 90 degrees waves.

H_s **= 3.5 m (Figure 7.7c and 7.7f)**: There is another decreasing trend for the minimum heave position. The pattern is similar to what was found before.

An overall conclusion can be drawn from the previous analysis and it reads as follows: an increasing H_s reduces the minimum heave position because of the bigger excitation, T_p = 9 seconds shows the biggest influence on AG's response, a bigger value for γ shows a smaller minimum heave position because there is more energy in the spectrum and the least variation is shown for wave directions above 105 degrees. Overall, to predict what would be happening to AG during operation, it is recommended to use the parameters in the ranges as shown in Table 7.3. A summary of the conclusion is given in Table 7.4.

Variable	Range	Unit
T_p	6.0 – 8.0	[s]
Wave direction	105 – 180	[degrees]
H_s	1.5 – 3.5	[m]
γ	2.5 – 3.5	[-]

Table 7.3: Parameter ranges, for T = 17m

Design variables		Conclusion
T_p	[s]	Big influence
Wave direction	[degrees]	Moderate influence
H_s	[m]	Moderate influence
γ	[-]	Slight influence

Table 7.4: Design variables, influence on heave motion

It is clear that the wave direction has an influence on AG's motions. The connection with the topside can be best predicted when the motions of the two bows are similar. The motions are closest to one another when experiencing head waves (180 degrees). Since this research goes through the research loops only once, this first estimation of AG's motions when lifting using QdB tanks only, is done for head waves.

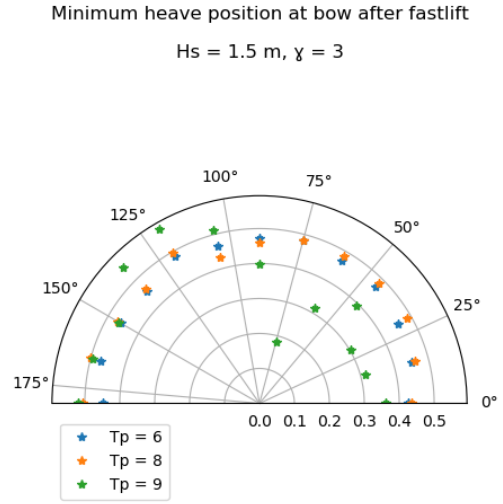

(a)

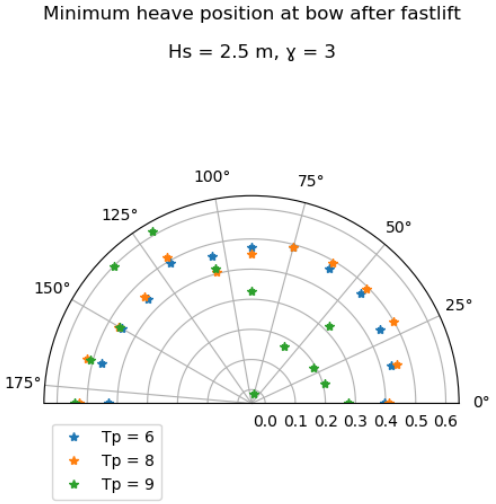

(b)

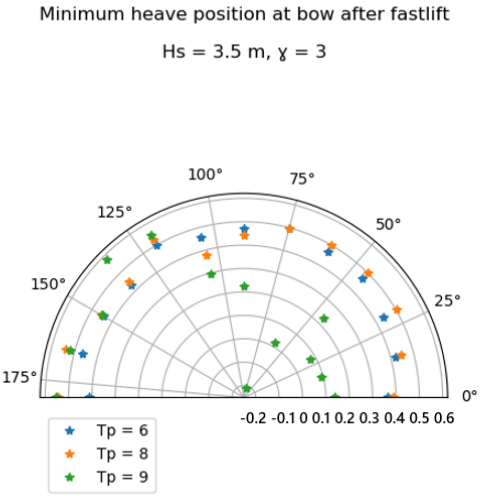

(c)

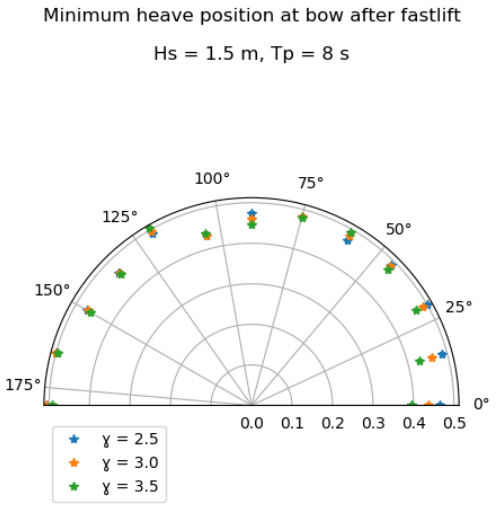

(d)

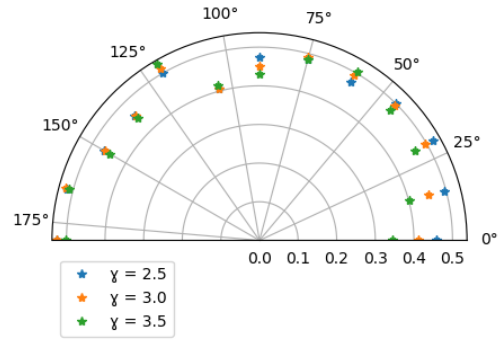

(e)

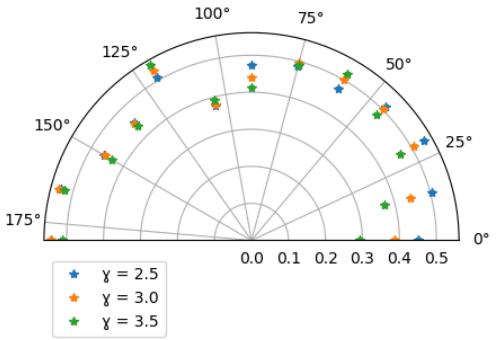

(f)

Figure 7.7: Sea state parameter analysis

7.4.2. Cummins' coefficients

The assumption was made to keep Cummins' coefficients constant for a change in draught. For a more accurate estimation of vessel motions, the mass matrix, the added mass, the damping through the impulse response function and the stiffness matrix change as a function of draught. This subsection discusses the sensitivity of the implementation of Cummins' equation when moving from 38 to 35.5 meters draught. For this analysis, the coefficients are changed for both draughts. A motion comparison by means of standard deviations shows the effect of the change. The QdB force is set to zero Newton to focus on vessel motions in a free floating condition.

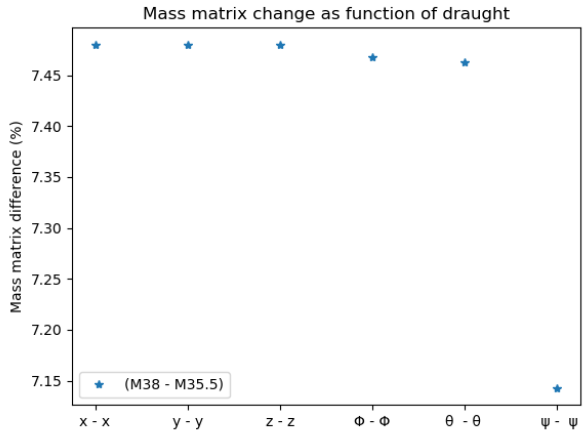

Figure 7.8: Mass matrix, T=35.5 and T=38 m

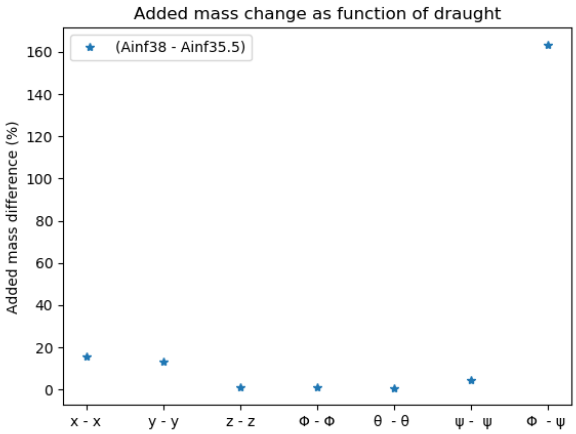

Figure 7.9: Added mass for freq. to ∞, T=35.5 and T=38 m

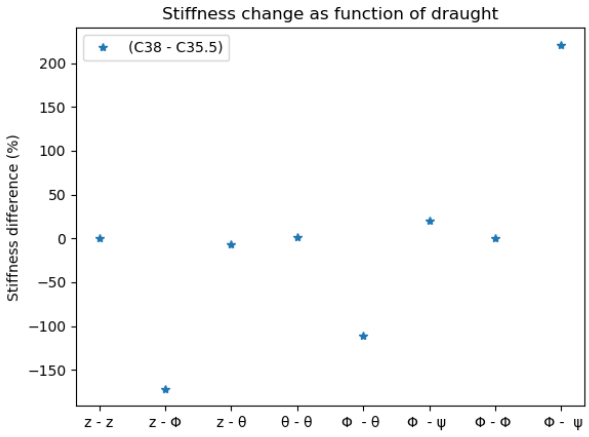

Figure 7.10: Stiffness matrix, T=35.5 and T=38 m

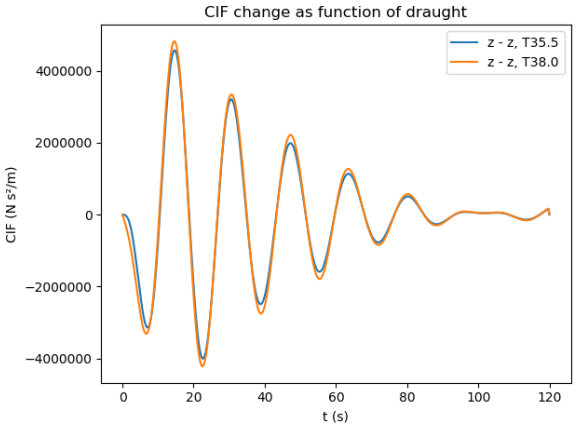

Figure 7.11: CIF (z - z), T=35.5 and T=38 m

Cummins' coefficients are plotted in Figures 7.8 - 7.11. From the mass- , the added mass- and the stiffness matrix, the stiffness matrix shows the biggest changes. The combination of pitch and yaw shows over 200% difference. The CIF matrix is plotted for heave. The difference between the areas under both graphs is roughly 32 percent. The next step is to see if these changes add up to a difference for the computation of vessel motions.

The standard deviations for the motions of the T = 35.5 meters and T = 38 meters draught are shown in Table 7.5. H_s = 2.5 meter, T_p = 8 seconds, γ = 3.3 and head waves are applied. Except for roll, all motions are of the same order of magnitude. Since roll is of such a small value, the difference is not taken into account. This means that for future operations in the range of 35.5 - 38.0 meters draughts, the coefficients can be kept a constant value.

	T = 35.5 m	T = 38 m	
	σ		
x	4.17	3.93	[m]
y	$4.99 \cdot 10^{-8}$	$3.74 \cdot 10^{-8}$	[m]
z	0.0099	0.0064	[m]
ϕ	$3.19 \cdot 10^{-10}$	$4.30 \cdot 10^{-11}$	[rad]
θ	$4.61 \cdot 10^{-5}$	$3.07 \cdot 10^{-5}$	[rad]
ψ	$1.82 \cdot 10^{-10}$	$1.91 \cdot 10^{-10}$	[rad]

Table 7.5: Motion comparison

7.5. Feasibility QdB system

For the QdB system to be feasible, the pretension- and fast lift phase (Section 1.1.3) need to be studied. The pretension study includes the rebounce at the connection plateau. For fast lift, rebounce of the jacket after lifting the topside needs to be prevented.

7.5.1. Pretension

During pretensioning, the maximum heave amplitude is of interest. The maximum heave amplitude is applied to the connection plateau. To get a statistical value of the heave amplitude at the bow for the implemented Cummins' equation, the simulation is ran 900 times for T = 38 meters, H_s = 2.5 meters, T_p = 8 seconds and γ = 3.3. The QdB force is set to zero Newton to focus on vessel motions in a free floating condition. A histogram of the maximum heave amplitude is generated per time series (Figure 7.12).

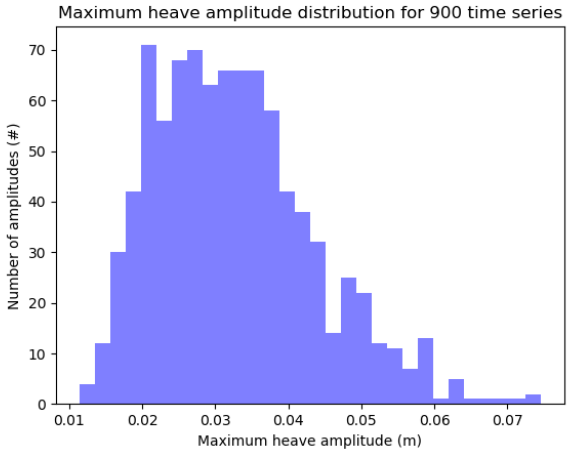

Figure 7.12: Probability of maximum single heave amplitude

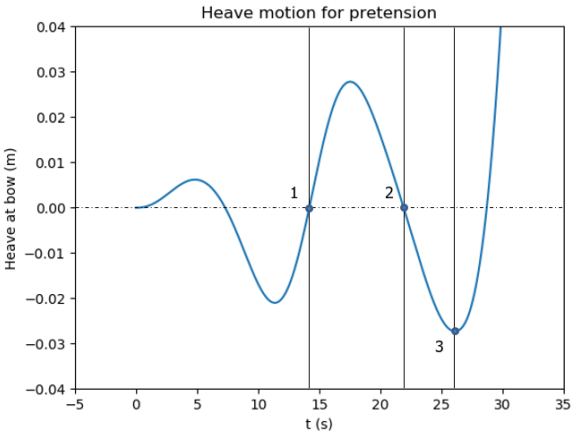

Figure 7.13: Pretension

The 0.028 m single heave amplitude is chosen to be most probable. This is done by considering the histogram a Rayleigh distribution. The amplitude is applied to the connection plateau (Figure 7.13). For the current model, 12 seconds is needed to empty out the volume of water being equivalent to the topside's weight. The fast lift can start at 26 seconds (Figure 7.13, (3)) when having a first connection at 14 seconds (Figure 7.13, (1)). The question is whether the system starts lifting between 1 and 2 of Figure 7.13 and if the system loses contact between 2 and 3.

The first part of the question is answered by comparing the stiffness of AG in heave direction to the stiffness defined by the topside's weight (including a safety factor of 1.1) and the distance of 0.028 meter (ζ_{heave}). Equation 7.22 shows that AG would not be lifting the topside between 1 and 2 of Figure 7.13 because AG's stiffness is smaller than the topside's stiffness. There is an initial impact when connecting to the topside. Possible rebounce from this impact is not studied in this work.

$$
\begin{aligned}
AG_{C_{heave}} &\leq \frac{Topside_m \cdot 1.1 \cdot g}{\zeta_{heave}} \\
AG_{C_{heave}} &\leq \frac{Topside_m \cdot 1.1 \cdot 9.81}{0.028} \\
6.2 \cdot 10^8 &< 2.77 \cdot 10^{10} \qquad [N/m]
\end{aligned} \tag{7.22}
$$

The second part of the question is on AG losing the connection with the topside. The estimation is that AG would not lose contact between 2 and 3 since 2/3 of the topside's mass is already transferred to AG at 2. It is recommended to investigate this further since the topside is not added to the model.

7.5.2. Fast lift

The time series belonging to the pretension plot as shown in the previous subsection is plotted in Figure 7.14. According to the design requirements, both castellation and the safety margin need 0.5 meter (Section 4.5). The 0.5 and 1.0 meter are marked in Figure 7.14. Due to inertia, AG needs part of the safety margin at the beginning of the time series before converging to the 'above 1.0 meter' mark. This means that the topside will not hit the jacket after fast lift. The QdB system is said to be feasible for the fast lift part.

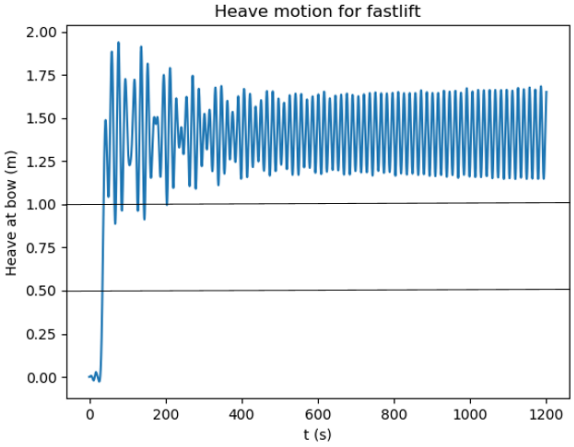

Figure 7.14: Fast lift

7.6. Chapter review

Vessel motions are calculated by including AG's mass, inertia, added mass, damping and stiffness. The dampening of the vessel is estimated by computing the radiation force with a time history. Diffraction forces and the QdB force excite the vessel. The motions for both bows are closest to one another when experiencing head waves. This research provides a first indication on the possibility to apply QdB tanks for lifting. Head waves can be applied for this purpose. It is assumed that for a draught of 35.5 - 38 meter, the coefficients of Cummins' equation can be kept constant. Only a slight difference would occur when applying coefficients as a function of draught in this range. The QdB system shows to be feasible for pretension since AG will not lift the topside at this point. Impact is not included in this study. For fast lift the QdB system is feasible since the topside will not hit the jacket after the lift. To improve the procedure by reducing the required volume of water, the application of trim can be studied.

8

Applying trim during fast lift

It is clear that the QdB system is feasible when applying the QdB force for heave only. An improvement to the procedure would be to apply trim for QdB. This introduces a possibility to reduce the required volume of water and the amount of valves needed to lift the topside, making the system less complex. This chapter investigates the option to improve the procedure by applying trim during fast lift. Trim is applied during fast lift in stead of pretension or the combination of the two phases. By doing so, an uneven load distribution among the connection points of AG to the topside by means of trimming during load transfer is prevented. Throughout the chapter, comparisons are given to show the differences in motions for a relocation of the QdB force vector (Figure 8.1).

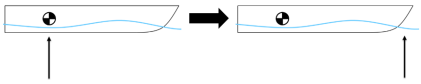

Figure 8.1: Relocation of the QdB force vector

8.1. Relocation of the QdB force vector, a comparison

When positioning the full QdB force at AG's COG, the required heave (Figure 8.2, convergence above 1.0 meter) is achieved although the volume of water and the amount of valves are high (Table 8.1). By relocating the QdB force vector whilst reducing the volume which is released during the fast lift, it is possible to apply trim (Figure 8.3). The total required volume of water is shown in Table 8.2. This is a reduction compared to Table 8.1. For a reduced volume of water, the amount of valves reduces as well since the emptying out of the tank is done within a constant time duration compared to the heave-only concept.

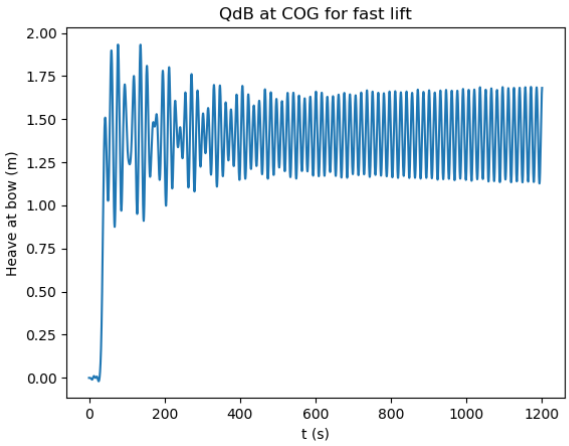

Figure 8.2: Heave at bow for QdB at COG

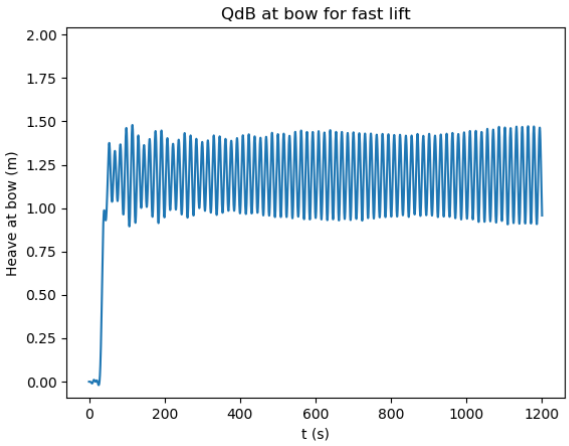

Figure 8.3: Heave at bow for QdB at bow

Required volume	$2.3 \cdot 10^5$	$[m^3]$
Valves	500	[#]

Table 8.1: System characteristics, COG

Required volume	$1.5 \cdot 10^5$	$[m^3]$
Valves	327	[#]

Table 8.2: System characteristics, COG and bow

8.1.1. Maximum allowable trim

A maximum of 1.5 meter trim per AG's length is allowed for as shown in Section 4.5. For a bigger trim, the TLS could not withstand the loading in AG's longitudinal direction. When applying the QdB force at the bow, the maximum relative heave between COG and the bow is roughly 1.2 meter (Figure 8.4). Assuming the COR to be at COG, this leads to a total trim of 1.9 meters (Figure 8.5).

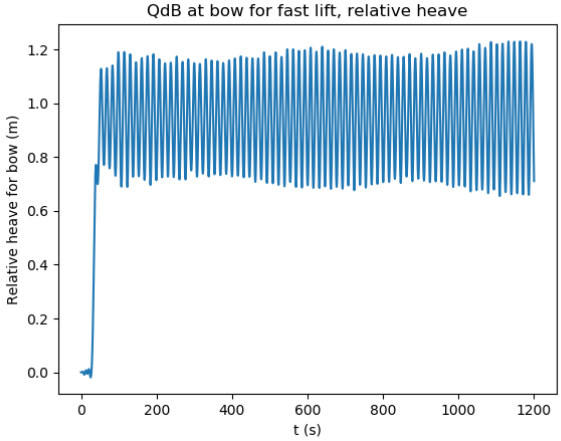

Figure 8.4: Relative heave at bow

Figure 8.5: Trim per length AG

When applying the QdB at the bow, the total trim over the length of AG exceeds the allowable trim since 1.9 > 1.5 meter. The next step is to reduce the trim by splitting the QdB force at the bow (Figure 8.6).

8.2. Another relocation of the QdB force vector

Another relocation of the QdB vector results in the separation as shown in Figure 8.6. The numbers (1) and (2) indicate the steps in which should be deballasted. (2) is deballasted during fast lift.

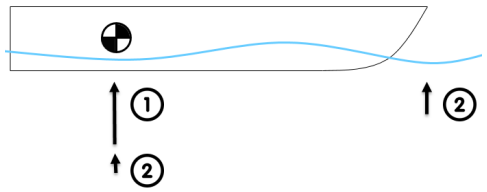

Figure 8.6: Split QdB, in two steps

When aiming for the trim to be of a maximum of 1.5 meters, the relative heave at the bow may be of a maximum of 0.95 meters (Figure 8.8). Cases 1 - 3 provide an overview of the effect of the change in volume released during fast lift to the trim per length of AG (Table 8.3). It is clear that a bigger released volume causes the trim to be bigger. The position of the QdB force vectors is kept the same for all cases. In terms of relative heave, and therefore trim, the third case would be the most ideal. The relative heave's maximum is barely exceeded (Figure 8.12). This case shows that roughly one third of the safety margin is needed (Figure 8.11: between the '0.5 meter' and '1 meter' mark), which is unfavourable. The least ideal case, in terms of trim, is the first case (Figure 8.8). A big exceedance is shown although the safety margin is not needed at all (Figure 8.7). To reduce the amount of safety margin needed for counterbalancing the limited trim exceedance, the second case is presented. The second case shows that it is possible to use only a limited part of the safety margin whilst letting the trim exceed its maximum slightly (Figures 8.9 and 8.10).

Case #	Volumes [m^3]		X-location at bow	Trim per length
	COG	Bow	from COG [m]	AG [m]
Case 1	$8 \cdot 10^3$	$1.5 \cdot 10^4$	255	1.9
Case 2	$7 \cdot 10^3$	$1.3 \cdot 10^4$	255	1.7
Case 3	$6 \cdot 10^3$	$1.2 \cdot 10^4$	255	1.5

Table 8.3: Used volume for step 2 of deballasting and obtained trim

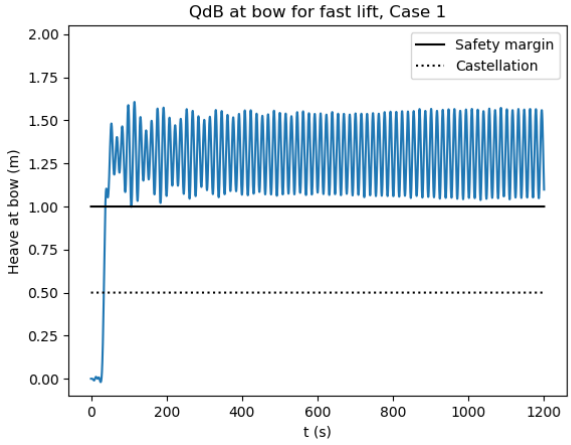

Figure 8.7: Heave for split QdB, Case 1

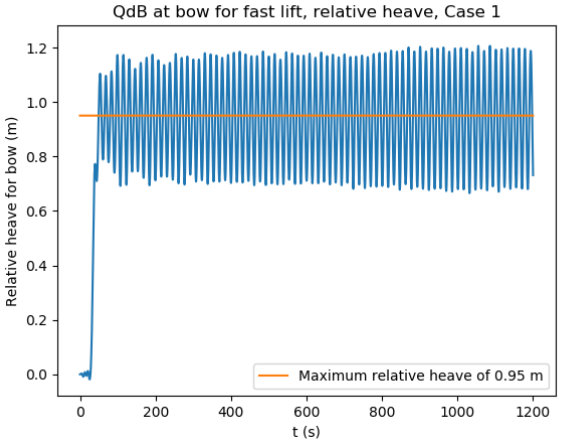

Figure 8.8: Relative heave for split QdB, Case 1

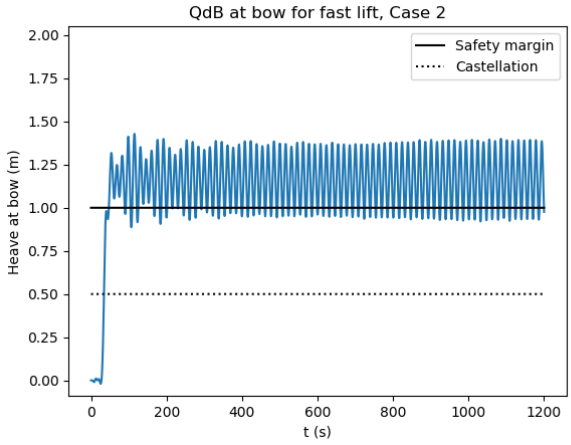

Figure 8.9: Heave for split QdB, Case 2

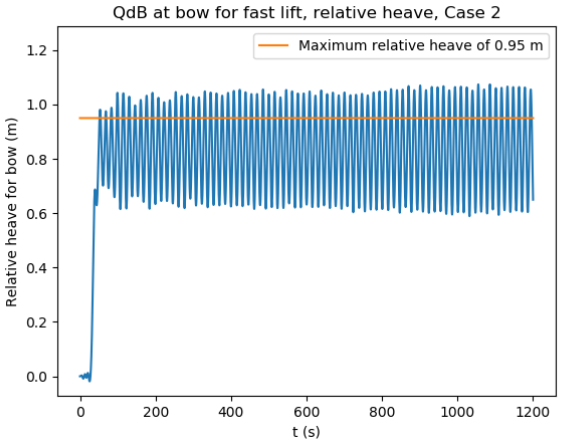

Figure 8.10: Relative heave for split QdB, Case 2

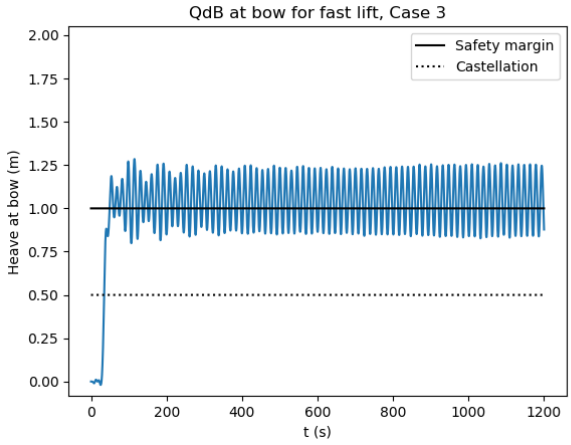

Figure 8.11: Heave for split QdB, Case 3

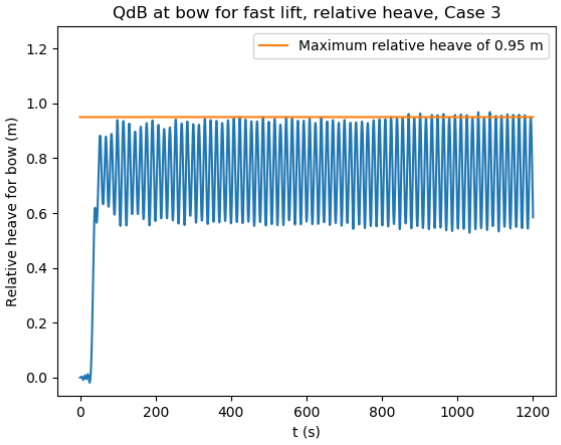

Figure 8.12: Relative heave for split QdB, Case 3

For the full heave at the bow to be roughly above 1.0 meters (castellation + safety margin) and the relative heave to exceed its maximum just slightly, the required volume and the volumes needed for step two of the QdB (Figure 8.6) are given in Table 8.4 for case 2. A slight increase of the required volume compared to Table 8.2 comes along with a slight increase of the amount of valves. This is still an improvement when comparing it to the 'QdB at COG only' concept (Table 8.1).

Required volume	$1.6 \cdot 10^5$	$[m^3]$
QdB 2, bow	$1.3 \cdot 10^4$	$[m^3]$
QdB 2, COG	$0.7 \cdot 10^4$	$[m^3]$
Valves	348	[#]

Table 8.4: System characteristics, Case 2

The plots in Figures 8.9 and 8.10 show that part of the safety margin is needed and that the trim will exceed its maximum slightly due to an exceedance of the maximum relative heave. When considering the 1.5 meter trim to be conservative, above plots conclude that it is possible to apply trim. Applying trim will simplify the complexity of the QdB system due to a reduction of the number of valves and a smaller required volume of water.

8.3. Chapter review

As the previous section describes, the application of trim during fast lift improves the procedure since the required volume of water and the number of valves are reduced. Applying trim simplifies the complexity of the QdB system by reducing the amount of valves by one third. It is recommended to apply trim during the fast lift although the total trim over the length of AG slightly exceeds the allowable trim. This is shown by through the maximum relative heave between the bow and the COG. If the exceedance of 0.2 meter is taken into account for a future TLS design, the QdB system is said to be feasible. It is recommended to further investigate the reduction of trim by spreading the tanks more.

9

Conclusions and Recommendations

This chapter gives an overview on the conclusions, answering the research questions. The conclusions lead to recommendations for future research. The research questions are first repeated as shown below:

(1.) ***"What are the design requirements for the QdB system?"***

(2.) ***"Is it possible to lift topsides using QdB tanks?"****

*It is possible to lift topsides using QdB tanks when stated that the QdB concept is feasible.

9.1. Conclusions

(1.) The first research loop is the quasi static analysis. This loop provides a first indication on whether the system is feasible or not. To provide this first indication, the design requirements read as follows: **a clearance of 1.5 meters, including a safety margin, castellation and a heave amplitude of 0.5 meter each, is needed to avoid rebounce of the jacket after lifting, pretensioning needs to be done within 1.5 peak period (= 12 seconds) of the waves, the heeling angle should remain zero degrees and the TLS allows for a maximum of 1.5 meter trim per AG's length**. A rough indication is given on the QdB's feasibility by showing that $2.3 \cdot 10^5 m^3$ water, 500 valves and 50 seconds are needed to heave AG 2.5 meters upwards and to lift the topside of 72,000 tons. The assumption is made that all external influences on the system are set to zero. The assumption is valid for a first indication and the system shows to be feasible. In reality waves will influence AG's motions. The next step is to include wave excitation in the model.

The linear superposition method is the second research loop. This method is used to give a first estimation on AG's motions in waves. The method is linear, which means that only small angled motions can be derived. No mass, added mass, damping or stiffness of the vessel are included. In reality AG's inertia causes AG to respond slower to deballasting than is modeled for superimposed motions. Since timing with respect to connecting AG to the topside is important, a more accurate dynamic model with respect to the previously named coefficients of the equation of motion is required. A better understanding of QdB's feasibility, providing details on both connecting to the topside and rebounce of the jacket after lifting the topside, is needed.

(2.) Vessel motions are calculated by applying the equations of motion through Cummins' equation. This is the third research loop. The dampening of the vessel is estimated by computing the radiation force with a time history. Diffraction forces and the QdB force excite the vessel. The motions for both bows are closest to one another when experiencing head waves. This research provides a first indication on the possibility to apply QdB tanks for lifting. Head waves can be applied for this purpose. It is assumed that for a draught of 35.5 - 38 meter, the coefficients of Cummins' equation can be kept constant. Only a slight difference would occur when applying coefficients as a function of draught in this range. The QdB system shows to be feasible for pretension since AG will not lift the topside at this point. Impact is not included in this study. For fast lift the QdB system is feasible since the topside will not hit the jacket after the lift. **Overall, the QdB concept is feasible when applying the QdB force for heave only.**

(2.) Previously, only heave was applied for lifting using the QdB system. The application of trim during fast lift improves the procedure of lifting since the total required volume of water and the number of valves are reduced. The number of valves goes down from 500 to 348. Applying trim therefore simplifies the complexity of the QdB system. It is highly recommended to apply trim during fast lift although the total trim over the length of AG slightly exceeds the allowable trim by 0.2 meter. An exceedance of the allowable trim could cause the TLS system to not withstand forces in AG's longitudinal direction. **If the slight exceedance in trim is taken into account for a future TLS design, the QdB system is said to be feasible when applying trim.**

9.2. Recommendations

For the one tank model, the extra frictional coefficient for streamline- and valve flow reduction needs to be elaborated to get a better understanding of the coefficient's application for the model of emptying a tank. Apart from this coefficient, the sensitivity on using bigger volumes than modeled for with the one tank model should be studied.

A second time going through the research loop of the quasi static analysis needs to focus on reducing the amount of valves to create a simpler system which is most probably less sensitive to fail. The fail safety of the system needs to be studied for a reduced amount of valves.

A better spreading of the tanks according to an actual tank plan could increase the efficiency of applying trim during fast lift using the implemented Cummins' equation. It is recommended to split the QdB force vector into multiple vectors. All the vectors can be given a new position. Running the simulation would give an estimation on the response of AG to the newly placed force vectors. When splitting up the tank in multiple tanks, emptying in multiple steps should be considered to be able to stop the process if this is required. To optimize the positioning of the tanks and AG's structural response, in terms of bending moments for instance, an optimization tool should be built.

For dynamic positioning (DP), thrusters are used to keep AG in place. When releasing roughly $2.3 \cdot 10^5 m^3$ water (or $1.6 \cdot 10^5 m^3$ for the trim concept), there is a large flow of water just underneath AG. This flow could influence the functionality of the DP thrusters. For future development, it is recommended to study the flow of the volume of water and to see if this can be incorporated in the tank positioning optimization tool.

For more details on rebouncing during the pretension phase, counter forcing from the topside needs to be included to address impact loading. More details should be provided on rebouncing by including a study on energy dissipation and/or absorption. It is also recommended to add the topside to the model to be sure that AG will not lose contact from the topside when heaving downwards during pretensioning.

For a future detailed design phase, it is recommended to take ballast water management into account by applying filters for instance. The tanks need to be kept clean from aquatic species as specified by IMO in their guidelines [16].

A

QdB concepts

Concept 1 – Basic
The first concept, Figure A.1, is based on the current design of the QdB tanks. The inlets (both for water and aeration) and outlet are butterfly valves. A rectangular tank is filled up by means of a pump for water supply. The main ballast system and a hand-pump are used as a back-up for the system. An extra outlet is added for an extra back-up option. This is different from the current design. Hydraulics are used to control the system.

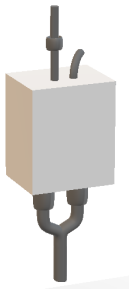

Figure A.1: Concept 1 – Basic

Concept 2 – Sliding Plate
The second concept uses a sliding plate as in- and outlet (Figure A.2, left side), being mechanically controlled. A cylindrical tank (Figure A.2, right side) introduces the possibility of using a pressurizing unit to pressurize and discharge water from the tank. For big tanks, pressurizing units with large diameters will be needed. This results into an upper limit of water volume per tank. The tank is filled by submerging the tank. The advantage to this technique is that no pumps are required. The disadvantage might be the duration of filling the tanks. Aeration of the tanks is done by pumping in pressurized air. The back-up of this system includes a hand-pump as well as the main ballast system.

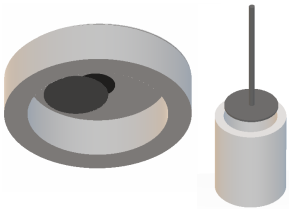

Figure A.2: Concept 2 – Sliding Plate

Concept 3 – Butterfly - Door
The third concept, Figure A.3, introduces the combination of butterfly valve as inlet and a door as outlet. The amount of hydraulics needed for this system is reduced compared to what is needed for Concept 1 since only the inlet requires hydraulics. The outlet is controlled by using a mechanical system. The standard rectangular tank is used in combination with pumps to supply water. To aerate the tanks a butterfly valve is opened. The back-up consists out of a hand-pump and the main ballast system.

Figure A.3: Concept 3 – Butterfly - Door

Concept 4 – Sliding Plate - Door
The fourth concept combines a sliding plate (Figure A.4, left side) as inlet with a door as outlet (Figure A.4, right side). This provides the use of mechanical controlling for both the in- and the outlet. A basic rectangular tank is filled using a pump to supply the water. Aeration is covered by opening a sliding plate. The main ballast system can be used as a back-up for discharging the tank. Apart from the main ballast system a hand-pump will be installed for the back-up.

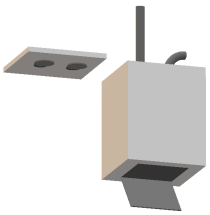

Figure A.4: Concept 4 – Sliding Plate - Door

Concept 5 – Door - Sliding Plate
The last concept, Figure A.5, uses a small door-valve as an inlet and a sliding plate as an outlet. These components can be controlled mechanically. The tank is cylindrical, using a suction unit to fill the tank (Figure A.2, right side). An upper limit of water volume per tank will be reached, being a result of using the suction unit. The same unit is used to pressurize and discharge the water from the tank. The aeration of the tanks is done by opening a sliding plate. This concept is not connected to the main ballast system, having only an extra outlet as a back-up.

Figure A.5: Concept 5 – Door - Sliding Plate

B

Motion Report

Motion Response Calculator - results form

General		
Date	25-Sep-2019	
Project	project name	
Specification	project specification	
Originator	Originator	
Revision	01	
Vessel	*Amazing Grace*	[-]
Draft	*17*	[m]
AQWA *.lis file	*BC_LOWFREQ.LIS*	[-]
Water depth	1000	[m]
Operational / survival condition	Operational	[-]
Wave spectrum	Jonswap	[-]
Wave directions	[180]	[deg]
Peakedness factor (γ)	3.3	[-]
Significant wave height	[ ]	[m]
Wave period	[6]	[s]
Wave period type	Tz	[-]
Wave height reduction applied?	no (default)	[-]

Location of interest*

	x-Coor [m]	y-Coor [m]	z-Coor [m]
test2			

Remarks

*Coordinate system
- positive x-axis points from the APP towards the bow
- positive y-axis points from CL towards PS
- positive z-axis points from the keelline orthogonal upwards
- 0 degree wave direction coming form the stern, positive defined anti-clock wise.

3 hours maximum, single amplitude motions and corresponding environmental conditions

Position**		x	y	z	rx	ry	rz	Hs [m]	Tz [s]	γ [-]	Wave Dir. [deg]
Surge	[m]	**0.07**	0.00	0.34	0.00	0.06	0.00	2.5	6	3.3	180
Sway	[m]	0.07	**0.00**	0.34	0.00	0.06	0.00	2.5	6	3.3	180
Heave	[m]	0.07	0.00	**0.34**	0.00	0.06	0.00	2.5	6	3.3	180
Roll	[deg]	0.07	0.00	0.34	**0.00**	0.06	0.00	2.5	6	3.3	180
Pitch	[deg]	0.07	0.00	0.34	0.00	**0.06**	0.00	2.5	6	3.3	180
Yaw	[deg]	0.07	0.00	0.34	0.00	0.06	**0.00**	2.5	6	3.3	180

Velocity**		x	y	z	rx	ry	rz	Hs [m]	Tz [s]	γ [-]	Wave Dir. [deg]
Surge	[m/s]	**0.05**	0.00	0.24	0.00	0.04	0.00	2.5	6	3.3	180
Sway	[m/s]	0.05	**0.00**	0.24	0.00	0.04	0.00	2.5	6	3.3	180
Heave	[m/s]	0.05	0.00	**0.24**	0.00	0.04	0.00	2.5	6	3.3	180
Roll	[deg/s]	0.05	0.00	0.24	**0.00**	0.04	0.00	2.5	6	3.3	180
Pitch	[deg/s]	0.05	0.00	0.24	0.00	**0.04**	0.00	2.5	6	3.3	180
Yaw	[deg/s]	0.05	0.00	0.24	0.00	0.04	**0.00**	2.5	6	3.3	180

Acceleration**		x	y	z	rx	ry	rz	Hs [m]	Tz [s]	γ [-]	Wave Dir. [deg]
Surge	[m/s^2]	**0.05**	0.00	0.17	0.00	0.03	0.00	2.5	6	3.3	180
Sway	[m/s^2]	0.05	**0.00**	0.17	0.00	0.03	0.00	2.5	6	3.3	180
Heave	[m/s^2]	0.05	0.00	**0.17**	0.00	0.03	0.00	2.5	6	3.3	180
Roll	[deg/s^2]	0.05	0.00	0.17	**0.00**	0.03	0.00	2.5	6	3.3	180
Pitch	[deg/s^2]	0.05	0.00	0.17	0.00	**0.03**	0.00	2.5	6	3.3	180
Yaw	[deg/s^2]	0.05	0.00	0.17	0.00	0.03	**0.00**	2.5	6	3.3	180

**Remarks
- listed values for motions,velocities and accelerations are single amplitudes
- all values are related to 3 hours maxima
- for a complete description of the model and calculation method see the motion report.
- the gravity contribution [g*sin(phi)] is incorporated in all affected values
- Motion analyzer rev. 11

Figure B.1: Motion Report Allseas

Bibliography

[1] K.M. Adams. *Non-functional Requirements in Systems Analysis and Design*. Springer, USA, 2015. Chapter 2: Design Methodologies.

[2] J. Wang A.J. Mokashi and A.K. Vermar. A study of reliability-centred maintenance in maritime operations. Paper, School of Engineering, Liverpool John Moores University and Indian Institute of Technology, January 2002.

[3] Author:Unknown. Topsides, 2012. URL `https://www.2b1stconsulting.com/topsides/`.

[4] Prof.dr.ir. J.A. Battjes. *Vloeistofmehanica – Collegehandleiding*. TUDelft, Faculteit Civiele Techniek en Geowetenschappen, Subfaculteit civiele techniek, Sectie Vloeistofmechanica, 1999. Niet-stationaire stromen – page 7-10.

[5] W. L. Oberkampf C. J. Roy. A comprehensive framework for verification, validation, and uncertainty quantification in scientific computing. Paper, Aerospace and Ocean Engineering Department, Virginia Tech and Consulting Engineer, Georgetown, Texas, March 2011.

[6] IH Cantabria. Simplified numerical model for wecs, 2012. URL `http://www.bcamath.org/documentos_public/archivos/actividades_cientificas/TalkBCAMWSonCM20131018Armesto.pdf`.

[7] Peter R.N. Childs. *Mechanical Design Engineering Handbook*. Elsevier, 50 Hampshire Street, 5th Floor, Cambridge, MA 02139, United States, 2019. 1.5 Double diamond.

[8] W.E. Cummins. The impulse response function and ship motions. Paper, Institut für Schiffbau der Universität Hamburg, January 1962.

[9] S.J. Boyes M. Elliott D. Burdon, S. Barnard. Oil and gas infrastructure decommissioning in marine protected areas: System complexity, analysis and challenges. Paper, Institute of Estuarine Coastal Studies, University of Hull, UK, October 2018.

[10] G. Chen S. Lim S. Wang D. Zhao, Z. Hu. Nonlinear sloshing in rectangular tanks under forced excitation. Paper, Shanghai Jiao Tong University, School of Engineering Newcastle University, Marine Design and Research Institute of China and Jiangsu University of Science and Technology, December 2017.

[11] DNV. Modelling and analysis of marine operations, rule 8.3.2.8. Paper, DNV, April 2011.

[12] Ir. F. de Wit Dr. M. Tissier, Prof. A. Reniers. *Ocean Waves, Lecture Slides, lecture 2*. Delft University of Technology, Delft, 2018. Time-domain approach (wave-by-wave analysis), slide 5.

[13] H. Hatecke H. Dankowski. Stability evaluations of semi-submersible heavy transport vessels by a progressive flooding simulation tool. Paper, Institute of Ship Design and Ship Safety Hamburg University of Technology, July 2012.

[14] J. Lee H. K. Lim. On the structural behavior of ship's shell structures due to impact loading. Paper, Hyundai Mipo Dockyard Co. and School of Naval Architecture and Ocean Engineering, University of Ulsan, May 2017.

[15] Y. Zhao H. Liu, J. Xiong. Three-dimensional behavior of embedded anchor lines under out-of-plane loading. Paper, Tianjin University and Shanghai Jiao Tong University, October 2018.

[16] IMO. Ballast water management - bwm convention and guidelines, 2019. URL `http://www.imo.org/en/OurWork/Environment/BallastWaterManagement/Pages/Default.aspx`.

[17] F. del Jesus A. Iturrioz I.J. Losada J.A. Armesto, R. Guanche. Comparative analysis of the methods to compute the radiation term in cummins' equation. Paper, Environmental Hydraulics Institute, "IH Cantabria", Universidad de Cantabria, C/Isabel Torres n 15 Parque Cientifico y Tecnologico de Cantabria, Spain, December 2015.

[18] W.W. Massie J.M.J. Journée and R.H.M. Huijsmans. *Offshore Hydromechanics Third Edition (2015)*. Delft University of Technology, Delft, 2015. Degrees of Freedom Ship, page 1-3.

[19] W.W. Massie J.M.J. Journée and R.H.M. Huijsmans. *Offshore Hydromechanics Third Edition (2015)*. Delft University of Technology, Delft, 2015. Hydrodynamic Loads, pg 7-4 – 7-5.

[20] W.W. Massie J.M.J. Journée and R.H.M. Huijsmans. *Offshore Hydromechanics Third Edition (2015)*. Delft University of Technology, Delft, 2015. Motions Superposition, page 6-5.

[21] W.W. Massie J.M.J. Journée and R.H.M. Huijsmans. *Offshore Hydromechanics Third Edition (2015)*. Delft University of Technology, Delft, 2015. Standard Deviation, page 5-33.

[22] W.W. Massie J.M.J. Journée and R.H.M. Huijsmans. *Offshore Hydromechanics Third Edition (2015)*. Delft University of Technology, Delft, 2015. linear superposition, page 6-39.

[23] Z. Guo D. Jeng K. Shen, L. Wang. Numerical investigations on pore-pressure response of suction anchors under cyclic tensile loadings. Paper, Zhejiang University and Griffith University, September 2017.

[24] E. Alexandre K. Hessner S. Salcedo-Sanz L. Cornejo-Bueno, J.C. Nieto Borge. Accurate estimation of significant wave height with support vector regression algorithms and marine radar images. Paper, Department of Signal Processing and Communications, Universidad de Alcalá, April 2016.

[25] Dr. Ir. P. Naaijen. Course notes / reader motions and loading of structures in waves mt44020 2018-2019, 1.4 complex notation, December 2018.

[26] H. P. Willemsen P. S. Heerema, A. Horowitz. Stabilizing system on a semi-submersible crane vessel. Paper, United States Patent, June 1978.

[27] H. P. Willemsen P. S. Heerema, A. Horowitz. Stabilizing system for a crane vessel. Paper, United States Patent, January 1978.

[28] Mary Beth Privitera. *Contextual Inquiry for Medical Device Design*. Academic Press, Ohio USA, 2015. Developing Insights, Pg. 141-161.

[29] D. Ovalle R. Font, J. García. Modelling and simulating ballast tank blowing and venting operations in manned submarines. Paper, IFAC, September 2010.

[30] J. García R. Font. On a submarine hovering system based on blowing and venting of ballast tanks. Paper, Universidad Politécnica de Cartagena and DICA, August 2013.

[31] F. Rodenburg. Analysis of the structural integrity of a jacket during a decommissioning lift. Paper, TU Delft, October 2013.

[32] Allseas Group S.A. *common knowledge*. -, Delft, 2019. -.

[33] B. A. Foss T. I. Fossen. Sliding control of mimo nonlinear systems. Paper, Norwegian University of Science and Technology, March 1995.

[34] P. Tavi T. Korhonen. Automatic time-step adaptation of the forward euler method in simulation of models of ion channels and excitable cells and tissue. Paper, Institute of Biomedicine, Finland, April 2008.

[35] André van der Stap. Offshore engineering: intro current status and history – slide 18, 2017.

[36] Frank M. White. *Fluid Mechanics* 8^th *Edition in SI Units*. Mc Graw Hill Education, Rhode Island, 2016. Viscous Flow in Ducts – page 328 - 329.

[37] Frank M. White. *Fluid Mechanics* 8^th *Edition in SI Units*. Mc Graw Hill Education, Rhode Island, 2016. Table A.3 – page 739.

[38] W. J. Ko X. Wang. Study on submerging operation design for heavy-lift barges based on a real case analysis. Paper, Institution of MECHANICAL ENGINEERS, November 2017.

[39] Y. Zan F. Huang Y. Ma, L. Yuan. Numerical simulation of float-over installation for offshore platform. Paper, Harbin Engineering University and Springer-Verlag GmbH Germany, March 2018.

[40] X. Liu X. Wang J. C.P. Cheng Y. Tan, Y. Song. A bim-based framework for lift planning in topsides disassembly of offshore oil and gas platforms. Paper, Department of Civil and Environmental Engineering, The Hong Kong University of Science and Technology, March 2017.

[41] Z. Gao P. C. Sandvik T. Moan Y. Zhao, Z. Cheng. Numerical study on the feasibility of offshore single blade installation by floating crane vessels. Paper, AMOS, CeSOS, Department of Marine Technology Trondheim, Norway, March 2019.